SYNTHESIS AND CHARACTERIZATION OF DECANOIC ACID COATED MAGNETIC IRON (III) OXIDE NANOCUBES FOR THE PREPARATION OF UNIFORM NANOCUBE MONOLAYERS

Jennifer Eva Tasneem

A thesis presented to the faculty of Mount Holyoke College in partial fulfillment of the requirements for the degree of Bachelor of Arts with Honors

Department of Chemistry

Mount Holyoke College

South Hadley, Massachusetts

May 2017

This thesis was prepared under the direction of Dr. Himali

Jayathilake, for 8 credits of independent study.

ACKNOWLEDGEMENTS

TABLE OF CONTENTS

LIST OF FIGURES AND TABLES

Page
number

ABSTRACT

   While research into the synthesis and characterization of magnetic iron oxide nanospheres has been heavy, the study of different shapes of iron oxide, such as nanotubes, nanocubes, nanorods, etc. has not been thorough. In this project, we investigated the less common magnetic Fe_3O_4 nanocubes. These nanocubes were synthesized by the thermal decomposition of iron (III) acetylacetonate. The synthesis was carried out in the presence of decanoic acid as the surfactant and also the organic solvent dibenzyl ether. The presence of decanoic acid coated nanocubes were confirmed using Fourier Transform Infra-red (FTIR) Spectroscopy.

   Since iron oxide nanocubes are unstable in air and especially in solution, due to their high surface energy and tendency to aggregate, mixed solvent systems of different ratios by volume of chloroform to methanol namely, 1:4, 1:3, 1:2, 1:1, 2:1, 3:1, 4:1 were used as dispersing agents for the nanocubes with pure chloroform as a control. This was done to determine if mixed solvent systems would be able to prevent the formation of nanocube aggregates as opposed to single solvent systems.

   The decanoic acid coated nanocubes were analyzed under a Transmission Electron Microscope (TEM) which were deposited on carbon-coated TEM grids. These particles were deposited on the grids using two different techniques, the Langmuir-Schaefer technique at the air-water interface, as well as drop casting. Slope analysis of the isotherms obtained from Langmuir-Schaefer samples were performed to study phase transitions during sample preparation. The TEM grids for different samples were analyzed under the microscope to record images in order to study the behavior and morphology of the nanocubes. TEM analysis revealed that thin, crystalline packing of nanocubes could be achieved when the Langmuir-Schaefer technique was used with a chloroform:methanol ratio of 3:1. The size distribution of the nanocubes could be measured from TEM images and a pure chloroform sample was used to determine the average size to be 14.25 ± 4.04 nm which is quite close to the superparamagnetic limit of iron. From the results it could be confirmed that a mixed solvent system of chloroform and methanol is able to disperse decanoic acid coated nanocubes to reduce aggregation in solution and for the formation of crystalline packed layers and that thermal decomposition is a suitable method to synthesize uniform nanocubes with a narrow size distribution.

1. Introduction

1.1 Nanoparticles and Nanotechnology

Synthesis of nanoparticles has received a great deal of attention particularly in the last few decades. A reason for this is the unique properties of nanoparticles (NPs) and their diverse applications. Nanoparticles are particles of diameter between 1-100 nm. These particles have characteristic properties and behavior which differ considerably from their bulk materials. Therefore, owing to their small size and distinctive properties, nanoparticles have a wide variety of applications in biotechnology, catalysis, biomedicine, and data storage, etc.[1] Properties of nanoparticles can vary depending on their size, shape and compositions. At the nanoscale, the surface-to-volume ratio increases and the surface effects become more significant.[2] Hence researchers are interested in studying different shapes of NPs and also examine how modifying the surface chemistry, assembly, etc. can alter their properties.

1.2 Iron and Its Magnetism

Iron is among those materials, whose properties at the nanoscale deviate considerably from its bulk material counterpart.[3] Iron is a magnetic material however, for the most part, pure bulk iron is not magnetic. When the size of iron particles falls below 100 nm, the surface-area to volume ratio becomes very large and thus the mechanical and chemical properties of the material is significantly

affected.[4] Iron exhibits a type of magnetism called ferromagnetism also common to nickel and cobalt. The strength of magnetism of a material can be quantified using the magnetic dipole moment, μ, in a loop of current which is given by,

$$\mu = IA \tag{1}$$

where, A is the area of the enclosed loop and I is the current circulating in the loop. The quantum mechanical interaction of iron at the atomic level causes the spins of unpaired electrons to align themselves in a region known as the domain. In the bulk material, the magnetic domains orient themselves randomly in different directions which results in the material to be demagnetized and be magnetically inactive. In the presence of an external magnetic field, the magnetic domains align themselves parallel to each other causing the material to be magnetized.[5] After being subjected to an external magnetic field, the material tends to remain magnetized to a certain extent even after the removal of the external field. This phenomenon of "remembering its magnetism" is known as hysteresis and can remain indefinitely unless reversed. Demagnetization of the material can only occur by the application of the magnetic field in the opposite direction.[4]

1.3 Iron Oxide Nanoparticles

There are many different forms of iron-oxide nanoparticles but among the two main forms of iron oxide are magnetite (Fe_3O_4) and its oxidized form,

maghemite (γ-Fe_2O_3). There are also other forms of iron oxides which have been studied such as hematite (α-Fe_2O_3). Iron oxide nanoparticles are particles with a diameter under 100 nm. One of the main uses of iron oxide nanoparticles including nanocubes is in the field of magnetic data storage.[1] This application uses the unique magnetic property of iron oxide nanoparticles which is their superparamagnetic behavior. Among the different types of magnetism, paramagnetism occurs when materials are attracted by an external magnetic field to form induced, internal magnetic field in the same direction of the applied magnetic field.[6] In contrast, diamagnetism occurs when materials are repelled by an external magnetic field due to an induced magnetic field in the opposite direction of the applied field. Unlike paramagnetism and diamagnetism, superparamagnetism is a type of magnetic property that occurs in small ferromagnetic or ferrimagnetic nanoparticles.[7] In large magnetic materials, particles have multi domain structures as shown in Figure 1.[8] As the particle size reduces, the number of domains keeps decreasing, until a critical diameter of a few nanometers is reached which in iron is usually about 6 nm. At this size, the particle only has a single domain.[9] For such a small size when an external magnetic field is removed, the average magnetism of the particle is zero due to the cancellation of the spin up and down of magnetic spin and the particle is said to be in the superparamagnetic state. At this state, the presence of an external magnetic field can actually magnetize the particles sometimes stronger than an actual magnet however in the absence of a field, the magnetism is very unstable.

Changes in the magnetic coercivity, that is, the ability of iron oxide to withstand an applied magnetic field, shows fast response by superparamagnetic iron oxide nanoparticles.
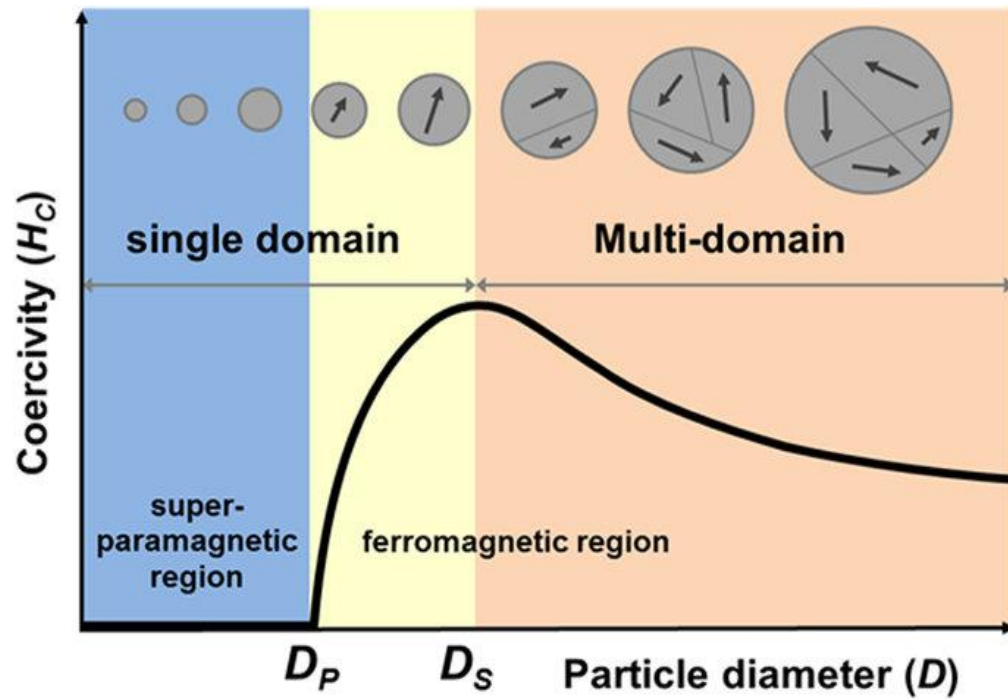
Figure 1: Coercitivity against nanoparticle radius to show the reduction of size of nanoparticles from multi-domain to single domain and to the superparamagnetic state.[8]

Along with the size, temperature also plays an important role in superparamagnetism. This is important for the purpose of magnetic data storage. Above a certain limit known as the blocking temperature, particles lose their stable magnetization and are unable to store data, thus application of iron oxide nanoparticles in magnetic data storage is challenging.[10]

1.4 Crystalline Structure

Maghemite and magnetite have very similar crystalline structure. The crystal structure of Fe_3O_4 follows a cubic inverse spinel pattern with alternating octahedral and tetrahedral-octahedral layers as shown in Figure 2(a). In the crystalline structure of Fe_3O_4, oxygen ions form a face-centered cubic (FCC) closed-pack lattice with both octahedral and tetrahedral interstitial sites occupied by iron. Specifically, half of the octahedral interstitial sites are occupied by divalent iron ions (Fe^{2+}) and the other half of octahedral sites and all tetrahedral sites are occupied by trivalent iron ions (Fe^{3+}).[11] At room temperature, electrons are free to move back and forth between Fe^{2+} and Fe^{3+} at the octahedral sites.
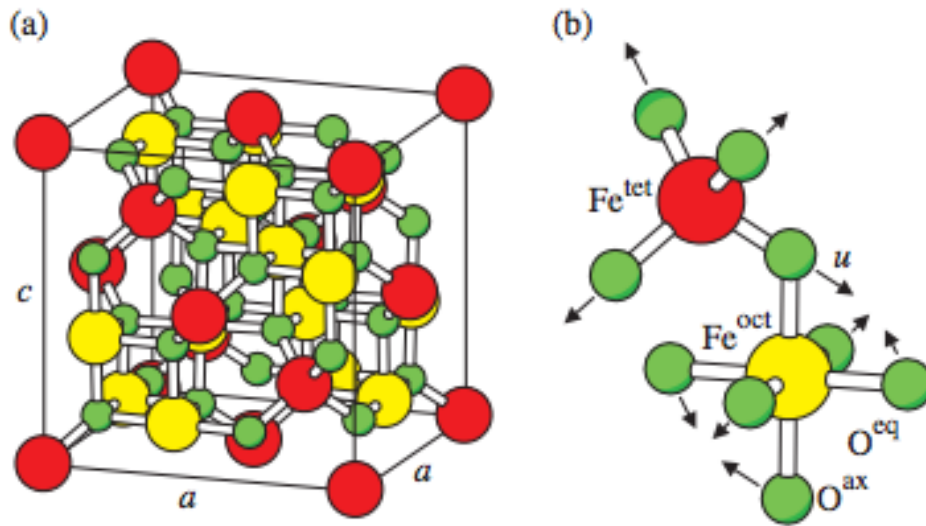
Figure 2: 2(a) [left] Crystalline structure of magnetite (Fe_3O_4) follows a face-centered cubic inverse spinel pattern. **2(b) [right]** Magnification of a tetrahedron and an adjacent octahedron sharing an oxygen atom.[12]

The main difference in the crystal structure of maghemite is the presence

of vacancies in some positions of Fe atoms as shown in Figure 3(b) as opposed to

the crystal structure of magnetite shown in Figure 3(a).[12] This results in reduction

of symmetry of the crystal structure. For this reason, Fe_2O_3 has lower magnetism

than Fe_3O_4 and studies have shown that the magnetism is actually ten percent

lower than Fe_3O_4.
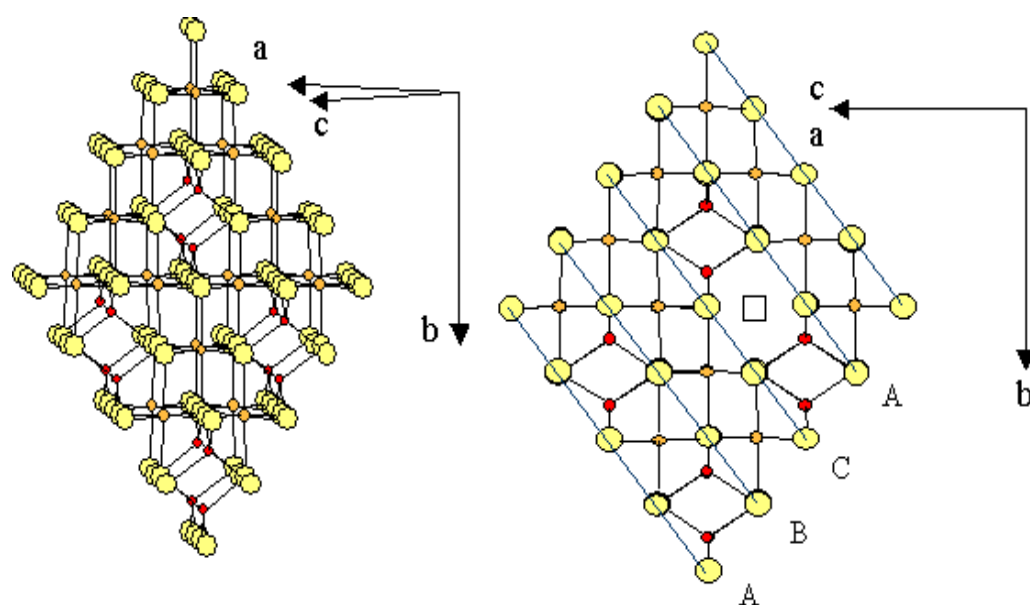
Figure 3: 3(a) [left] Crystal structure of Magnetite, Fe_3O_4 and **3(b) [right]** Maghemite, γ-Fe_2O_3.[12]

1.5 Why Study Iron Oxide Nanocubes?

Since the last two decades a lot of research has gone into the study of

spherical iron oxide nanoparticles. However, the studies of differently shaped

nanoparticles such as nanocubes, nanorods, etc. have been largely unexplored.[8]

The surface of nanoparticles can be functionalized with different molecules which

can alter the surface chemistry of nanoparticles. As the size of particles decreases

the surface effects become more significant. These differences in properties allow

the different applications of iron oxide nanoparticles. In particular, the synthesis

of iron oxide nanocubes (magnetite/maghemite $Fe_3O_4/\gamma\text{-}Fe_2O_3$) by thermal

decomposition of an organic iron precursor in a high boiling point organic solvent

yields highly crystalline magnetic nanoparticles with excellent magnetic

properties. Coprecipitation method on the other hand, can be used to produce NPs

of a wide range of sizes. However, these tend to show low magnetic properties

and tend to aggregate in the sizes required for biomedical applications.

1.5.1 Data Storage

One of the most important applications of magnetic nanoparticles is in

data-storage and our research focuses on synthesizing iron oxide nanocubes

suitable for data-storage applications. An individual nanoparticle can be used to

store a data bit with binary code 0 or 1 as shown in Figure 4.[5] Data can be stored

on a magnetic hard disk as a series of binary digits (0 or 1) patterned by reversal

of magnetization around a surface of a rotating disk. Currently, data on hard disk

is stored on a continuous magnetic film consisting of densely packed

nanoparticles on the surface. As shown in the gray image, each data bit consists of

about a 100 nanoparticles of sized ranging between 10-20 nm. The presence of a

magnetic reversal can exist in the area of one data bit which can represent the

presence of two different magnetizations within that area. The binary code '1' is

the presence of a reversal and '0' is the absence of a reversal and the orientation

of magnetization along an axis reflects the storage of data in the binary method.
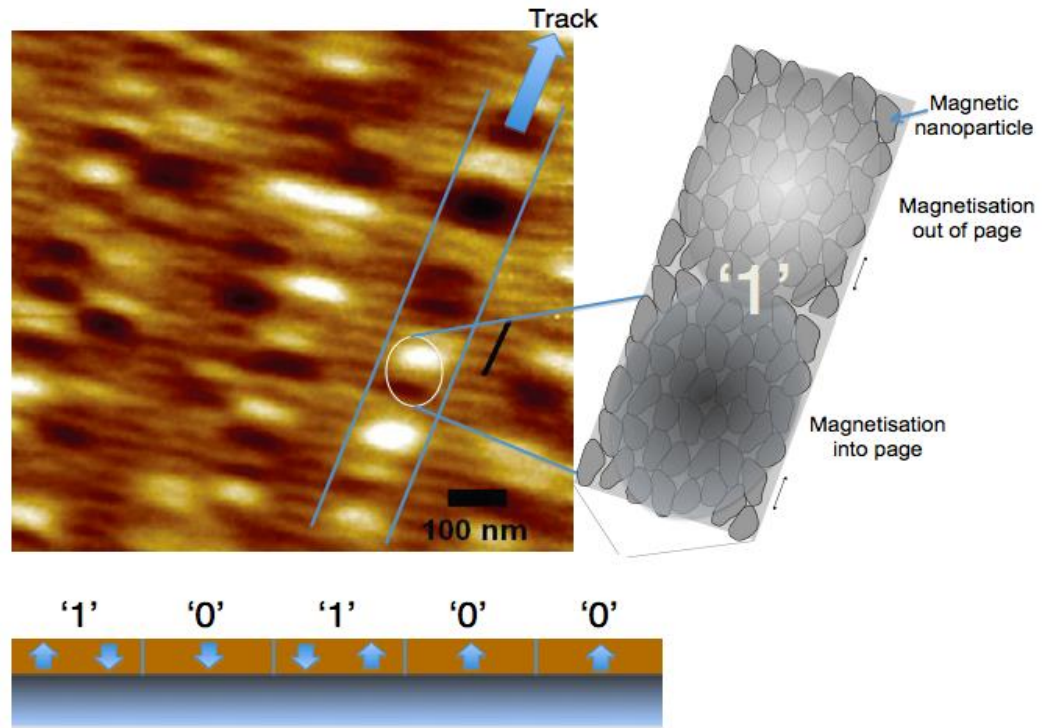
Figure 4: Atomic Force Microscope image of the magnetization pattern on the surface of a Momentus hard disk of size 394 Gigabyte/inch^2 disk. The disk consists of nanoparticles with size range of 10-20 nm.[5]
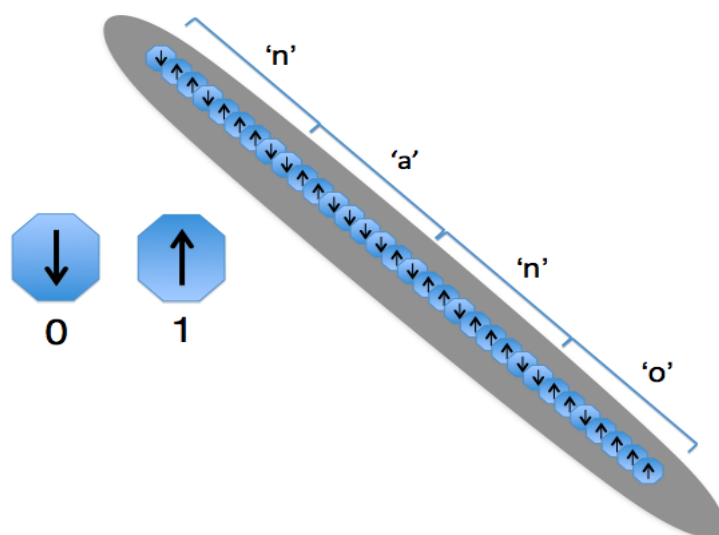
Figure 5: A hypothetical means of data storage on individual magnetic nanoparticles is shown. This way a large amount of data can be stored in a much more compact way.[5]

Figure 5 shows a hypothetical situation of storing larger amounts of data

on single nanoparticles. Instead of using hundreds of nanoparticles to store only a

single bit of data, a more efficient way to store data would be to use a single

nanoparticle to store one data bit as the above diagram illustrates. In this case, the

presence or absence of a reversal does not need to be considered. Since the

magnetization is oriented along a single axis, a magnetization with orientation

downwards (spin down) could be used to represent '0' and orientation upwards

(spin up) could represent '1'.[5] However, there are fundamental limitations that

need to be addressed as nanoparticles of a critical size are used for data storage.

The feasibility of this hypothesis is limited to a favorable synthesis and assembly

of these magnetic particles which can be accounted to optimizing synthesis

conditions as well as to develop a way of manipulating the assembly of particles for data storage.

1.5.2 Targeted Drug Delivery

A very interesting application of nanoparticles is in biomedicine.[2] Nanoparticles can be used to attach proteins, antibodies or drugs for targeted drug delivery. The magnetic core of the particle can be used to steer the attached molecule to specific areas of the body where the drug can be released. The attached molecule can thus be used to target specific cells for example cancer cells as shown in Figure 6. Traditional treatments of cancer such as radiotherapy or chemotherapy are able to kill cancer cells but at the same time they also affect healthy cells. Hence, targeted drug delivery can be more efficient for this purpose. However, this application requires particular size, charge and surface chemistry of the magnetic particles in order for it to be successful.

Iron oxide nanoparticles have low toxicity and are biocompatible which is why they are suitable for use inside the body. Due to the strong magnetic response in the presence of an external magnetic field and their stability in biological environment, superparamagnetic nanoparticles are important for biomedical applications.[13] After a suitable mode of entry into the body, for example intravenous injection, different sizes of nanoparticles can exit the body in slightly different ways. For example, particles with diameters greater than 200 nm are sequestered and isolated by the spleen and are removed from the body by

phagocytosis. Particles with diameters less than 10 nm usually undergo very rapid

renal clearance. Hence particles with sizes between 10-100 nm are ideal for drug

delivery as they have sufficient blood circulation times whilst having sizes that

allow penetration into thin blood capillaries to reach the desired tissues.
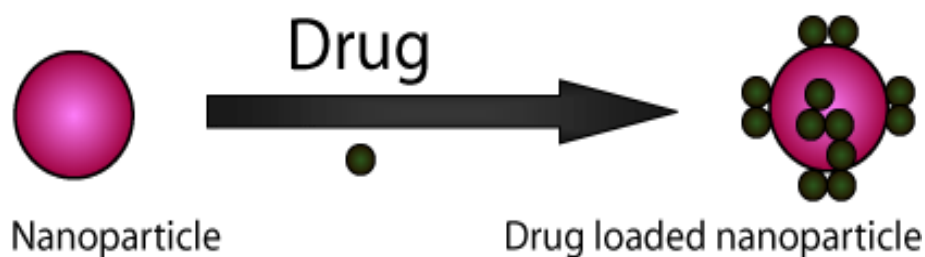
Figure 6: Mechanism of targeted drug delivery. The nanoparticle is loaded with molecules of the drug and targeted to specific tissues.[6]

1.5.3 Magnetic Resonance Imaging (MRI)

Another important biomedical application of magnetic iron oxide

nanocubes is as contrast agents in Magnetic Resonance Imaging (MRI).[14] As

opposed to paramagnetic particles, superparamagnetic iron oxide nanoparticles

can be functionalized and size-tailored in order to adapt to various kinds of soft

tissues. The particles can be coated with various polymers and polyelectrolytes for

stability in order to prevent agglomeration. MRI imaging depends on the

measurement of nuclear magnetic resonance (NMR) signals emitted from protons

in the human body when placed in an external magnetic field. In the presence of

iron oxide contrast agents, MRI performance is considerably improved as they

reduce the relaxation times of the NMR signals thus producing hypointense

(darker) images of the abnormalities in the MRI brain scan.

1.6 Synthesis of Magnetic Nanoparticles

Industrial application of magnetic iron oxide nanoparticles requires

uniform, monodisperse particles. Due to their highly unstable nature in air and in

solution, there are many challenges in obtaining suitable particles. One of the

most important challenges is optimizing experimental conditions leading to the

formation of high quality particles in order to have a reproducible process that can

be commercialized.[15] In addition to optimizing experimental conditions, another

challenge is to control the dipole-dipole interaction between the particles with

suitable stabilizing agents in order to prevent their tendency to aggregate into

clusters. Hence, a successful synthesis method is required to produce

monodisperse, shape-controlled particles that have a narrow size distribution.

1.6.1 Coprecipitation Method

The coprecipitation method is one of the oldest and most common

technique for the synthesis of commercial magnetic iron oxide nanoparticles as

MRI contrast agents.[6] This technique can be used to synthesize both magnetite

and maghemite nanoparticles. A base is added in an aqueous mixed solution of

Fe^{3+} and Fe^{2+}. This results in the formation of iron oxide precipitate. In order to obtain particles with good stability or solubility in solution, conditions such as the molar ratio of Fe^{3+}/ Fe^{2+}, synthesis temperature, synthesis time, type of salt and base used, and the pH value of the reaction mixture, can be altered to obtain particles with varying size, shape and composition of the particles.

Coprecipitation synthesis is very simple with mild reaction conditions and without the use of toxic reagents.[15] Due to this, the cost of synthesis is quite low allowing the procedure to be easily scaled up for the production of large yields of magnetic iron oxide nanoparticles which are often water soluble due to their hydrophilic surfaces. Even though the conditions for coprecipitation are well studied and optimized, the particles synthesized using this method have very irregular morphologies with non-uniform, polydisperse sizes.[15] Hence this makes these particles unsuitable for data storage and for drug delivery.

1.6.2 Microemulsion

Microemulsion is the isotropic and thermodynamically stable dispersion of two immiscible liquids.[6] The system is stabilized by surfactants which can form a monolayer and act as an interface between the two liquids. For microemulsions of water and oil, the hydrophobic tail of the surfactant molecules are dissolved in the oil phase and the hydrophobic part is in the aqueous phase. The diameter of the dispersion domain is usually between 10 and 50 nm but can vary depending on the molar ratio of water to oil.[13] For the synthesis of magnetic nanoparticles, two

similar microemulsions are combined so that collision, fusion and splitting, allow the two types of micelles to interact in order to allow the exchange precursors. As a result, precipitation of the nanoparticles occurs within the micelles that can be extracted by centrifugation after the addition of solvents such as ethanol. The microemulsion method requires large amounts of solvent for the extraction of particles.[13] In addition, particles are aggregated even in the presence of surfactants and it is quite difficult to produce particles of larger diameters with high yields making it unsuitable for industrial use.

1.6.3 Hydrothermal Synthesis

Hydrothermal synthesis occurs in an aqueous medium under a high temperature and vapor pressure in sealed containers, usually autoclaves. There are two main methods for hydrothermal synthesis. One of these methods for the synthesis of crystalline particles is a one step process without the use of surfactants. On the other hand, particles can also be synthesized using a surfactant and therefore the system contains a liquid phase as well as a solution phase which allows the interaction between the two phases. Previous research has shown that iron oxide particles synthesized using this method are highly crystalline and are able to exhibit superparamagnetic properties at room temperature.[2]

Apart from coprecipitation, microemulsion and hydrothermal synthesis, there are other methods of the synthesis of nanoparticles, including sol-gel method, hot injection, polyol method to name a few.[6] One of the most important

method is actually thermal decomposition of an organometallic compound.[16-17] Even though hydrothermal synthesis is able to produce particles with high quality and crystallinity, thermal decomposition works even better and is able to produce particles with higher yields and greater control.[18]

1.7 Thermal Decomposition for the Synthesis of Fe_3O_4 Nanocubes

Synthesis of magnetic iron (III) oxide nanocubes can be successfully carried out using thermal decomposition of organometallic compounds.[13] This process involves the decomposition of organometallic compounds in organic solvents like dibenzyl ether, dioctyl ether, etc. There are many types of organometallic precursors that can be used for the source of iron that include iron acetylacetonate ($Fe(acac)_3$), iron pentacarbonyl ($Fe(CO)_5$) and even iron ions Fe^{3+}. The reaction mixture also contains surfactants, also known as ligands or capping molecules, for stabilization; for instance, decanoic acid, oleic acid, lauric acid and octanoic acid are some examples of surfactants. Although the synthesis procedure is somewhat complicated, as it requires an inert atmosphere, requires high decomposition and reflux temperatures, and has long reaction periods, the size distribution of particles is considerably narrow, the yield of particles is high and it is possible to control the shapes of the nanoparticles during synthesis by varying different conditions quite easily.[13] Because of these advantages, thermal decomposition is chosen as the preferred method for the synthesis of the magnetic

Fe_3O_4 nanocubes. Figure 7 shows a typical reaction progression analyzed by transmission electron microscopy.
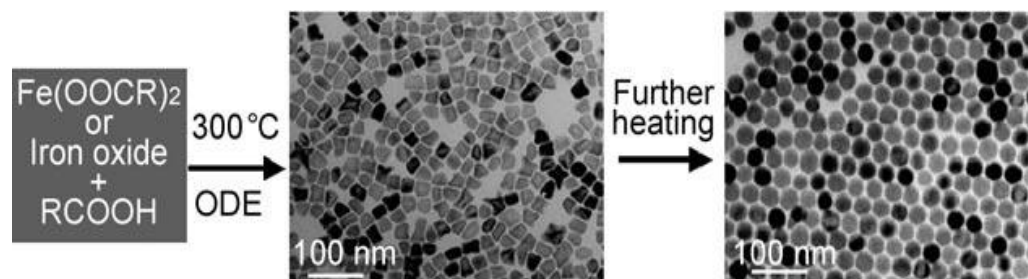
Figure 7: Synthesis and formation of iron oxide nanoparticles from different sources. Transmission Electron Microscopy images at different reaction times are shown. The image in the center shows the formation of cube like structures and further heating can convert these particles to uniform nanospheres.[22]

1.8 Controlling the Properties of Iron Oxide

Magnetic iron oxide nanoparticles tend to have high surface energies due to their large surface-to-volume ratio.[19] As a result, this leads to the formation of nanoparticle aggregates in order to counteract and minimize the surface energies. In addition, nanoparticles also tend to lose their magnetic and dispersing properties due to oxidation because of their high chemical activity.[4] These tendencies make it difficult for the regulation of the size, shape, stability and dispersibility of nanoparticles.
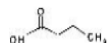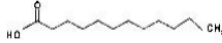
Different parameters used in the process of thermal decomposition can be varied to control the size, shape and uniformity of the nanocubes. For our

research, the iron source that was used iron acetylacetonate, $(Fe(acac)_3)$. The surfactant used was decanoic acid in an organic solvent of dibenzyl ether.

1.8.1 Effect of Surfactant Coating on Nanocube Size and Uniformity

One strategy to synthesize nanocubes of uniform size, shape and stability is to coat them with a suitable surfactant. If a suitable surfactant is used, it enables the particles to self-assemble with the desired arrangement and spacing. These protective shells not only stabilize the nanocubes, but also prevent external oxidation. A layer of surfactant can be adsorbed on the nanocubes causing them to have like charges depending on the type of surfactant used. As a result, there is electrostatic repulsion and thus the nanocubes are separated and evenly dispersed in the solution. There are various surfactants that can be used. Table 1 summarizes some surfactants which can be used for capping γ-Fe_2O_3 nanoparticles. The surfactant coating can also be done using polymers, fatty acids, inorganic layers, metal oxides or sulfides, etc.[5]

Table 1: Role of structure and length of carboxylic acid surfactant molecule on the γ-Fe_2O_3 nanoparticle size.[20]

Surfactant	Length of carbon chain	Structure	Molecule length[a]	Particle size	Inter-superlattice distance	Decomposition temperature
Butyric acid	C4			None		
Octanoic acid	C8		10.93 A	6 nm	2 nm	264 °C
Lauric acid	C12		17.8 A	9 nm	3.5 nm	280 °C
Oleic acid	C18		22.98 A	12 nm	4.5 nm	288 °C

[a]Calculated by Chem3D with molecular mechanics using MM2.

From the above table it can be noted that increasing the chain length of the acid surfactant molecules increases the size of the nanoparticles. Furthermore, studies have shown that the type of surfactant used can also affect the shape of the nanoparticles.[6] Another factor affecting the synthesis is the concentration of the surfactant. Generally, increasing the concentration of the surfactant acid increases the size of the nanoparticles as well as the uniformity resulting in bigger and highly self-assembled arrays of nanoparticles.

The concentration of the surfactant used can also play an important role during the synthesis procedure. Increasing surfactant concentration is able to produce particles that are larger and more uniform.[21] This is because, as the surfactant molecules coat the particles, they are more separated and stabilization of the particles contributes to increased monodispersity which in turn aids the assembly of the particles into uniform monolayers.

1.8.2 Effect of Temperature on Nanocube Size and Uniformity

In addition to the surfactants used in the experiment, there are various other factors affecting the synthesis of nanocubes. Among these, one of the most important factors is the decomposition temperature used during synthesis.[22] Studies have shown that a greater decomposition temperature typically results in a larger size of nanoparticles.[17] However, one disadvantage of using higher temperature is loss of uniformity in the sizes. Therefore, a lower temperature results in smaller, more uniform nanoparticles which interact more strongly with

the surfactant layer thus leading to the formation of homogenously dispersed solution.

Larger sizes of the carbon chain length of the surfactant require greater decomposition temperatures.[2] When using a carboxylic acid as the surfactant, with the increase in the length of carbon-chain, the catalysis of acid gradually becomes more insignificant as the dipole moment gets weaker and weaker, thus there is a need of higher decomposition temperature to bring reaction into completion.

In addition to the decomposition temperature, the heating rate plays a major impact on the shape and size of the particles.[5-7] Since nucleation of the particles occur at an early stage in the reaction, maintaining a uniform heating rate ensures that particles have a uniform size. If the heating rate is high, atoms continue to nucleate homogeneously and thus have a narrow size distribution.[17] On the other hand, if the heating rate is relatively low and allowed to fluctuate, a greater size distribution is observed due to an inhomogeneous growth.

1.8.3 Effect of Dispersing Agent

To ensure that the synthesized nanocubes can be preserved for long periods of time, it is important to stabilize them in a suitable dispersing agent. As iron oxide nanocubes are highly unstable in air and in solution due to their high surface energy, dispersing agents can stabilize particles by reducing their surface

energy. This can prevent further oxidation of the magnetite particles to maghemite and also prevent the aggregation of the particles. Additionally, the nanoparticles remain highly stabilized in solution because they have a surface that is mutually unreactive and repulsive toward other particles.[20]

In our research, a mixed solvent system of different ratios of chloroform and methanol is studied. Both chloroform and methanol are polar solvents with methanol having a greater polarity than chloroform. This system was chosen as the difference in polarity between chloroform and methanol that provides a unique balance of polarity that is favored by the nanocubes. Along with the solvents, the surfactant of choice, decanoic acid also provides a stabilizing effect as it coats each particle. An optimized dispersing agent system is yet to be determined that is suitable for the formation of monodispersed decanoic acid coated iron oxide nanoparticles that is free of aggregates.

1.9 The Project Goal

The goal of this study is to successfully synthesize uniform Fe_3O_4 nanocubes. Since nanocubes could be potentially be used for effective magnetic data storage, monodisperse particles of a narrow size distribution are required. Our goal is to synthesize particles with high crystallinity and monodispersity in order to ensure that particles have uniform magnetizations.
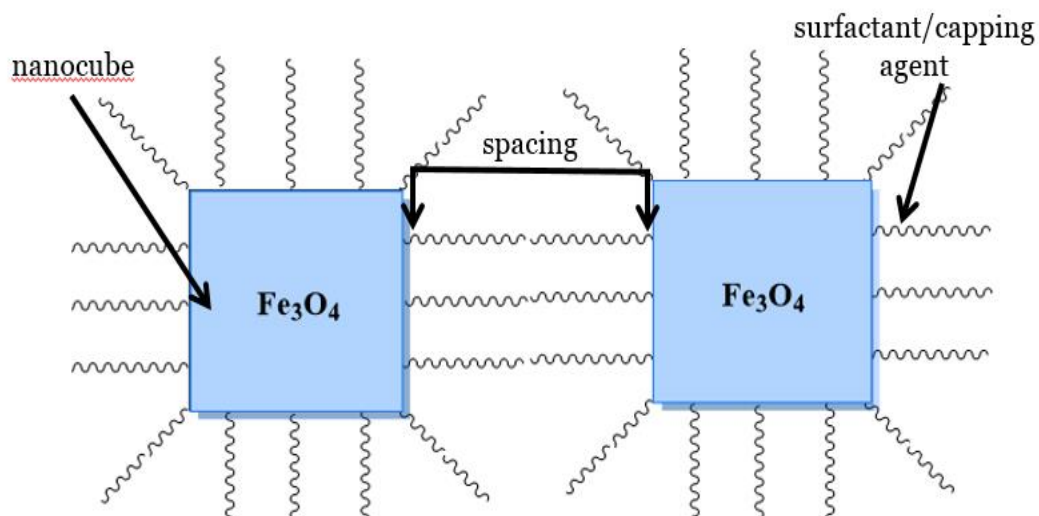
Figure 8: A schematic diagram showing the assembly of nanocubes.

The main goals of this study can be divided into four parts: first to successfully synthesis decanoic acid coated iron oxide nanocubes with controlled shape, size. Secondly, the synthesized nanocubes are dispersed in different ratios of chloroform and methanol along with pure chloroform to determine if mixed solvent systems perform better as opposed to single solvent systems. If the particles are successfully dispersed in the solvent system, uniform monolayers can be obtained using different deposition techniques on substrates. In this study, the nanocubes are deposited on substrates using two different techniques namely drop casting and Langmuir-Schaefer technique to understand their behavior and assembly.

Transmission electron microscopy (TEM) is used to analyze the samples dispersed in different ratios and study the two-dimensional assembly and surface

morphology of the nanocubes on the substrate. This is done in order to determine the ideal ratio of chloroform to methanol that is suitable for stabilizing the cubes. From the TEM images, the size of individual particles is measured and from these measurements the size distribution of the nanocubes is also determined.

2. INSTRUMENTAL METHODS

2.1 Preparation of Nanocube Thin Films

Nanocube thin films can be prepared using many different methods. There are four main techniques used to prepare nanocube films: drop casting, spin coating and two other techniques using a Langmuir trough, namely the Langmuir-Blodgett (LB) and Langmuir-Schaefer (LS) techniques. In this study, the substrate of choice is carbon-coated TEM grids. The preparation of stable, homogenous and well-packed particles is essential in the applications of nanocubes.

2.1.1 Drop Casting

Drop casting is one of the simplest methods for nanoparticle deposition on a substrate.[22] A very small amount of nanocubes in solution is pipetted using a micropipette on a substrate of choice, in this case a TEM grid, as shown in Figure 9. The substrate is left undisturbed for a few minutes to allow evaporation of the solvent. The solvent evaporates leaving a thin film of nanocubes on the substrate. Drop casting although simple, is also one of the most inefficient deposition techniques. This is because evaporation can result in greater aggregation of the cubes producing inhomogeneous films of nanocubes. However, drop casting is very useful for preliminary tests or when the homogeneity of thin deposit is not needed.
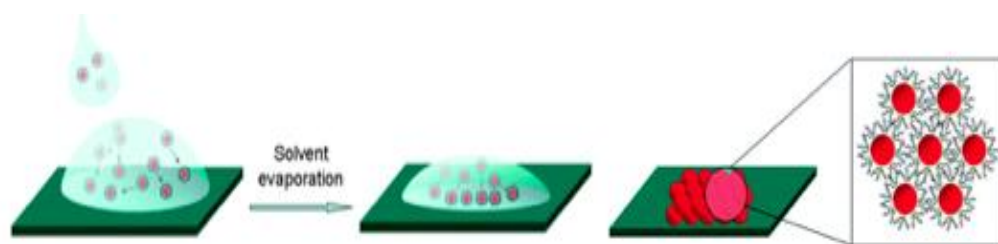
Figure 9: Deposition of nanoparticles on a substrate using drop-casting.[32]

2.1.2 Spin Coating

Another method of depositing nanocubes on a substrate is spin coating.[23] Spin coating is similar to drop casting, however the main difference is that the nanocube solution is deposited on a rotating substrate. In this method, a small piece of silicon wafer is placed on the spin coater. A substrate of choice, usually a carbon TEM grid is placed on the wafer. Before placing the grid, a small drop of water is pipetted on the surface to allow adhesion of the grid on the wafer surface. Like drop casting, a small amount of nanocubes in solution is pipetted using a micropipette on the TEM grid as shown in Figure 10. The centrifugal force resulting from the rotation of the spin coater causes the solution to spread and form a thin layer on the substrate as the solvent evaporates.[23] The formation of nanocube film depends on properties such as speed of spinning, temperature, nature of solvent and substrate, etc.
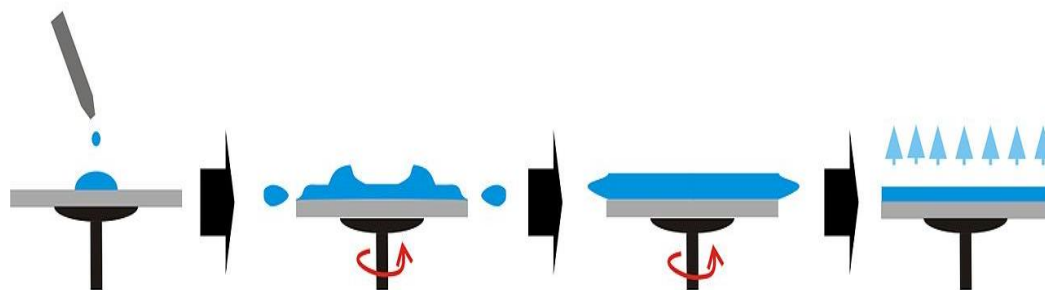
Figure 10: Deposition of a thin layer of nanocubes on a substrate using spin coating.[23]

2.1.3 The Langmuir Trough

The Langmuir trough is one of the most important aspects of our study. Two different deposition techniques can be performed using the Langmuir trough: the Langmuir-Blodgett and the Langmuir-Schaefer methods (Figure 11). However, for either of these techniques to be successful, it has to be ensured that the Langmuir trough is very clean.[24] Otherwise, dust particles can interfere with the formation of nanoparticle monolayer. For this purpose, solvents such as ethanol or chloroform can be used. Using a micro syringe, small volumes of the nanocube solution can be spread all over the water surface in the trough at the air-water interface. The layer is left to stabilize for a few minutes and to allow the evaporation of solvent.
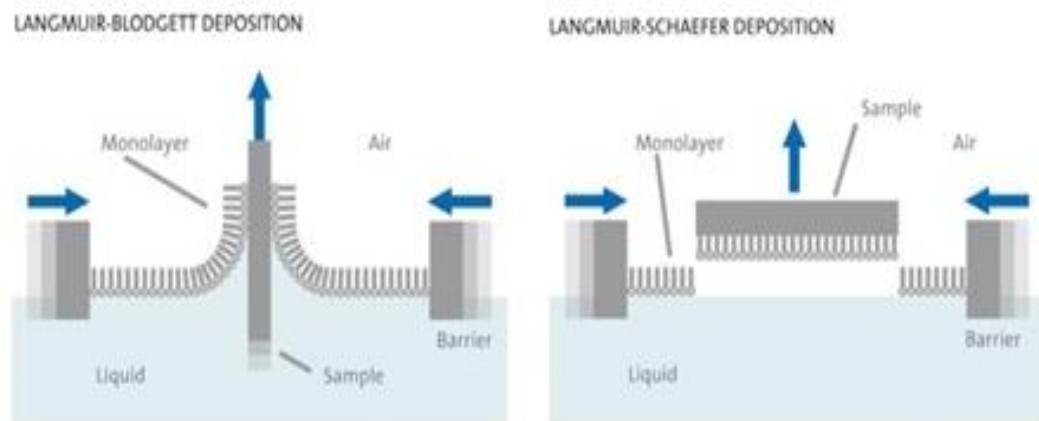
Figure 11: Schematic diagram of the Langmuir-Blodgett and Langmuir-Schaefer monolayer deposition techniques.[24]

An external force is applied to those floating surfactant molecules using the barriers in the Langmuir trough. With the barriers, the layer is compressed to allow the nanocubes to come close together to ensure packing of the nanocubes for the formation of a uniform monolayer of nanocubes. Compression of the nanocubes causes the monolayer to go through two-dimensional phase transitions which can be observed from the pressure-area isotherm.[24] The phase transitions are two-dimensional analogues to the gas, liquid and solid state of matter. The Wilhelmy plate suspended over the water surface measures the surface pressure and if the compression of the barriers is sufficient, a solid film will be created in the trough. Figure 12 shows the diagram of a typical isotherm. The nanoparticle films can be successfully studied if they reach the solid state. Langmuir trough deposition is traditionally carried out in the solid phase where surface pressure is high enough to ensure sufficient cohesion in the monolayer. This means that

attraction between the molecules in the monolayer is sufficient to prevent the

monolayer from falling apart during transfer to the solid substrate and ensures the

buildup of homogeneous multilayers through multiple depositions. At the solid

state, the monolayers can form highly self-assembled arrays with uniform

arrangement and spacing. On the other hand, at the liquid and gaseous states the

nanoparticles have uneven packing with large spacing. Even though it should be

ensured that that there is enough compression to allow the formation of a solid

monolayer, care should be taken to not allow extreme compression of the solid

state. This may cause the uniform packing of the nanoparticles to break and

eventually lead to the formation of multilayers of nanocubes as shown by the dip

in the isotherm.[27-28] A good isotherm can be typically used to clearly identify the

changes in the different states as it distinctly shows the phase changes through

changes in slope.
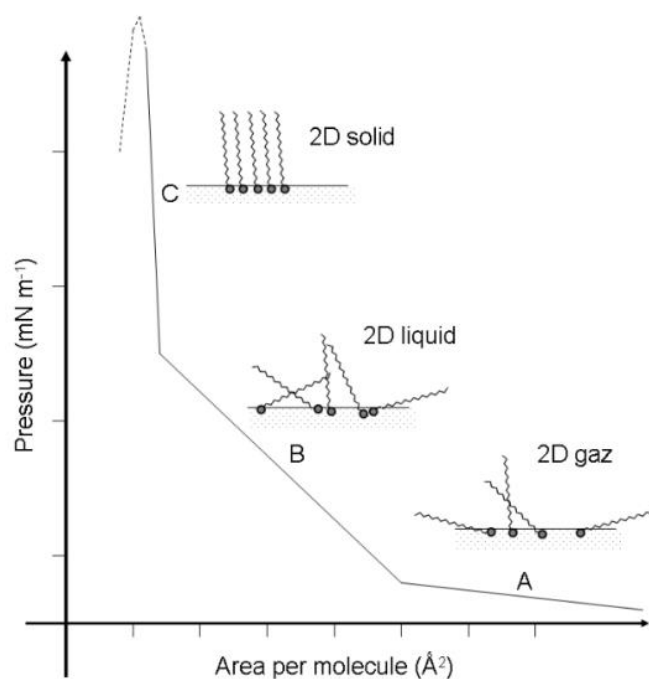
Figure 12: Schematic diagram of a surface pressure versus area isotherm.[25]

2.1.3.1 Langmuir-Blodgett Technique

Both the Langmuir-Blodgett and Langmuir-Schaefer techniques are useful techniques in the formation of controlled thin films at the air-water interface. The main difference between the two techniques is the direction of deposition of the substrate on the water surface. The Langmuir-Blodgett technique utilizes the vertical dipping of a substrate on the monolayer surface.[26] The substrate is gradually immersed into the nanocube surface and after the stabilization of the nanocube solution on the water surface, it is gradually extracted vertically from the water as illustrated in Figure 13. This leaves a layer of the nanocubes in

solution which is then allowed to dry and thus deposit a thin film of nanocubes on the surface of the substrate.
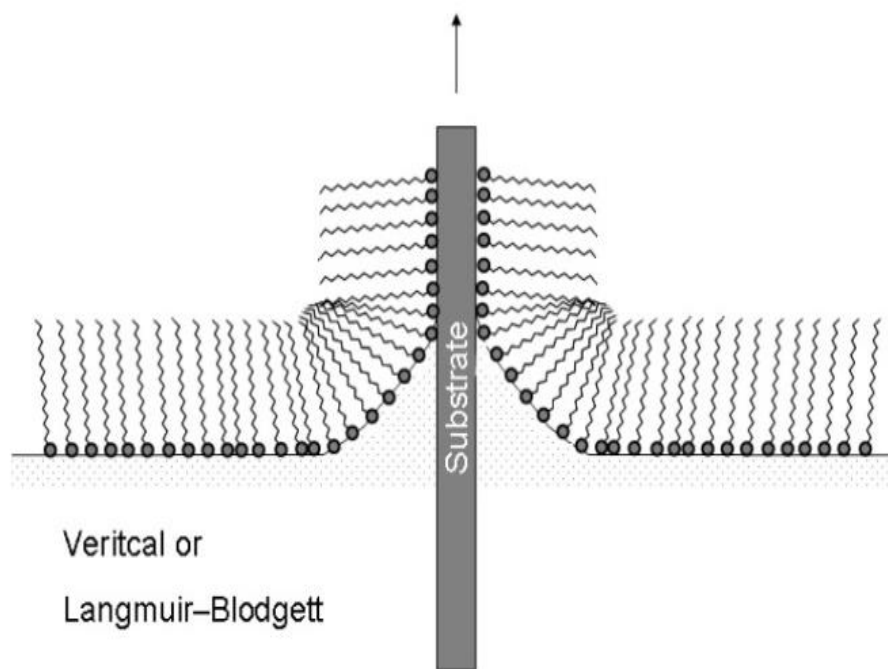
Figure 13: Schematic diagram of the Langmuir-Blodgett technique.[26]

2.1.3.2 Langmuir-Schaefer Technique

The Langmuir-Schaefer technique involves the horizontal deposition of the monolayer film on the substrate as shown in Figure 14.[7] In this method, after the compression and stabilization of nanocubes on the water surface, the substrate is carefully released horizontally on the dispersed nanocube surface to allow the transfer of the particles onto the substrate. The substrate is allowed to stabilize and finally extracted horizontally from the surface.
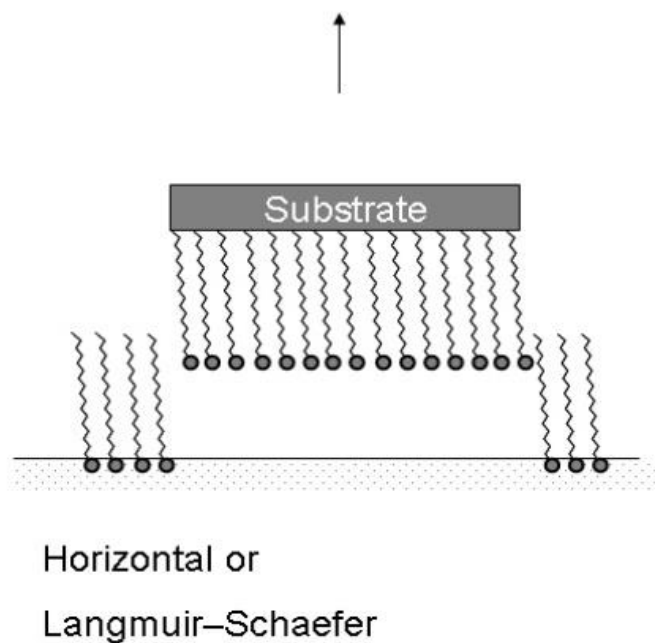
Figure 14: Schematic diagram of the Langmuir-Schaefer technique.[24]

2.1.3.3 Factors Affecting Langmuir Method

The LB and LS techniques are successful for the formation of uniform

monolayers however the efficiency of this depends on certain factors. After the

synthesis of the nanocubes, they are washed using a solution of hexane to acetone

of 1:1 ratio. The purification process is very important as it washes away any

residual surfactant, unreacted iron precursor and organic solvent.[28] For particles

with a wider size distribution, this washing process alone might not be sufficient.

The residual molecules in the nanoparticle solution can interfere with the

homogeneity of the monolayers and result in the formation of a heterogeneous

monolayer with broken areas. This means that the size distribution of the particles also plays a significant role during the packing process in the Langmuir trough.

2.2 Characterization of Nanocubes

2.2.1 Transmission Electron Microscopy (TEM)

The prepared thin films of iron oxide nanocubes on small carbon coated grids can be studied using a Transmission Electron Microscope (TEM) as shown in Figure 15.[29] In a TEM, electron beams are shot through the instrument onto the surface of the grid from the electron gun as a filament heats up. As the electron beam traverses, it passes through a series of lenses which scatter or diffract leading to the formation of an image. Contrasts in the image are produced by differences in electron beam scattering or diffraction formed between various elements of the microstructure or defect. As a result, the surface morphology and assembly of particles on the substrate can be observed. After passing through a series of lenses, the electron beam interacts with the sample, and a resulting beam is transmitted. The resulting scattering of electrons due to structural details on the grid surface can be projected on a florescent screen which can then be imaged to study the size and spacing of the particles using a software.

TEM is a vital characterization tool for directly imaging nanomaterials as it can be used to achieve and study the behavior of materials at very large magnifications.[30] This is essential in order to obtain quantitative measures of particle size, size distribution, morphology and also the behavior of grains.

Analysis of TEM images can be performed in order to measure the size of the

nanocubes to obtain quantitative results about their size distribution.
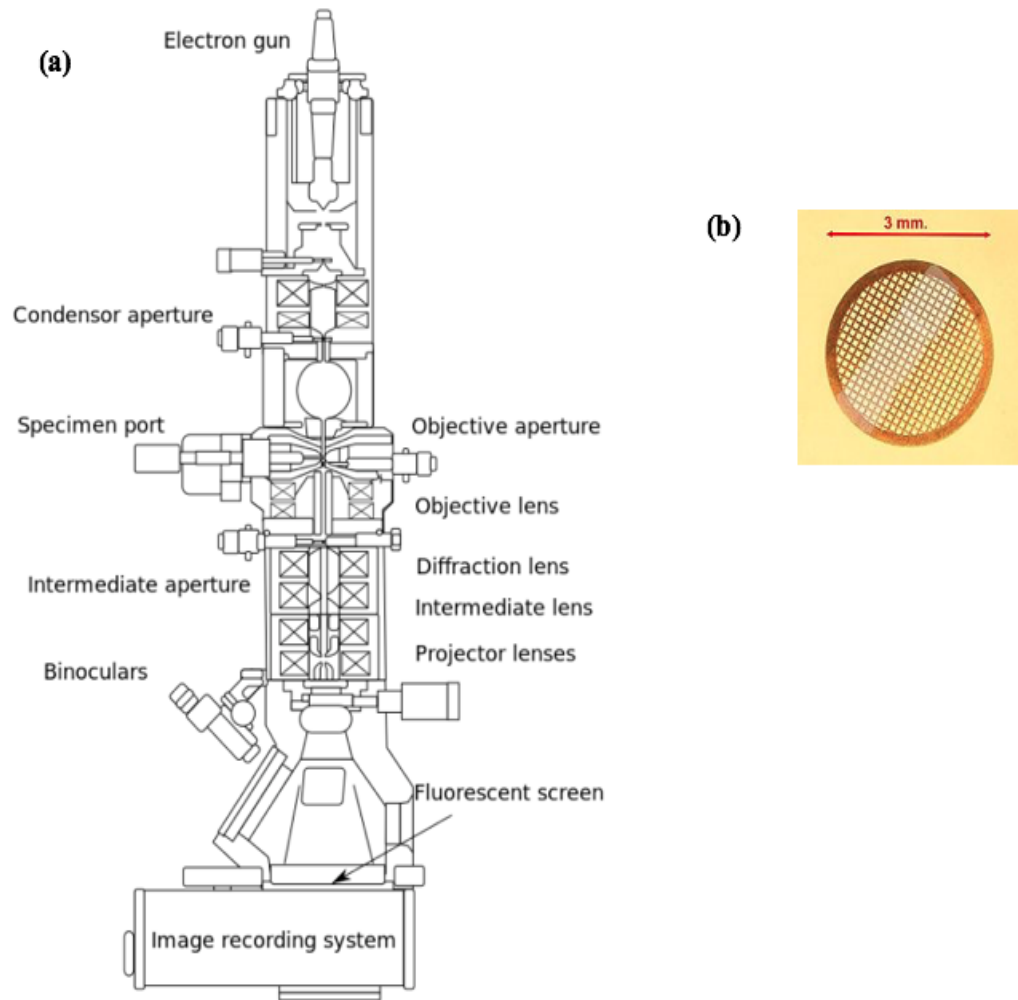
Figure 15: Left (a) The mechanism of a transmission electron microscope. **Right (b)** a TEM grid typically has a size of about 3 mm.[29]

During the image analysis of TEM since measurement of particles at the

nanoscale is involved, there are possibilities for errors in the measurement. A

reason for this is that when measuring size distributions, only a very small

sampling size is observed. A typical magnetic nanoparticles suspension composed of 10^{10} to 10^{15} particles/mL but on the other hand measurements of samples are done only for a few hundred (10^2) to thousand (10^3) particles.[31] Hence the sampling size is a number of magnitudes smaller than the actual amount of particles present in solution, and this gives us a very small sample pool to draw statistically conclusive remarks.

2.2.2 Fourier Transform Infra-red (FTIR) Spectroscopy

Fourier transform infra-red spectroscopy, FTIR samples can be extracted from the reaction mixture at different instances of time. FTIR analysis can be used to gain more insight into the formation and disassociation of certain bonds and functional groups. In traditional IR spectrometry, a sample is exposed to different frequencies of IR radiation. The spectra obtained tells us about the detected frequencies that are able to pass through the sample. FTIR on the other hand is able to collect electromagnetic spectral data in a wide range as it exposes the sample with many different frequencies simultaneously in a single light beam. By using a mathematical operation called the 'Fourier Transform', FTIR converts the raw data collected by the spectroscope into the desired spectrum to determine the frequencies that passed through the sample.[37] From this, a spectrum of Transmittance (%) against Wavenumber (cm^{-1}) is generated.

The FTIR at different reaction times can be analyzed to study peaks corresponding to the vibrational transitions characteristic of different bonds.

Bonds such as C=O, C-H and O-H bonds which are present in the surfactant, decanoic acid, show characteristic peaks. The appearance and disappearance of such peaks correspond to bond formations and disassociations as the reaction progresses. Therefore, by looking at the peaks on the spectra and their relative frequencies absorbed by each bond, FT-IR spectroscopy can be used to determine the presence of decanoic acid on the synthesized Fe_3O_4 nanocubes.

3. EXPERIMENTAL

3.1 Synthesis Procedure of Crystalline, Monodisperse Fe₃O₄ Nanocubes

Dibenzyl ether, decanoic acid, iron acetylacetonate (Fe(acac)₃) were obtained from Sigma-Aldrich and used without further purification. The heating source for the synthesis was a sand bath, which was set up prior to the reaction. To synthesize the iron oxide nanocubes, the dry reactants were added and mixed in the reaction vessel. The structures of chemical reagents are shown in Figure 16 and the setup of the synthesis apparatus is shown in Figure 17. A constant nitrogen flow was maintained into the vessel to keep the synthesis environment inert.
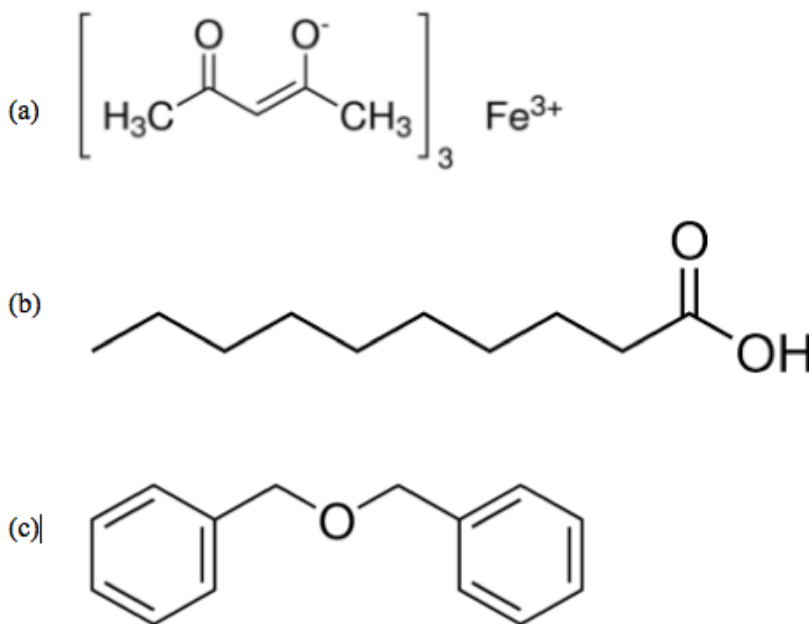

Figure 16: The chemical structures of the reagents used in the synthesis of Fe₃O₄ nanocubes: (a) iron acetylacetonate (b) decanoic acid (c) dibenzyl ether.
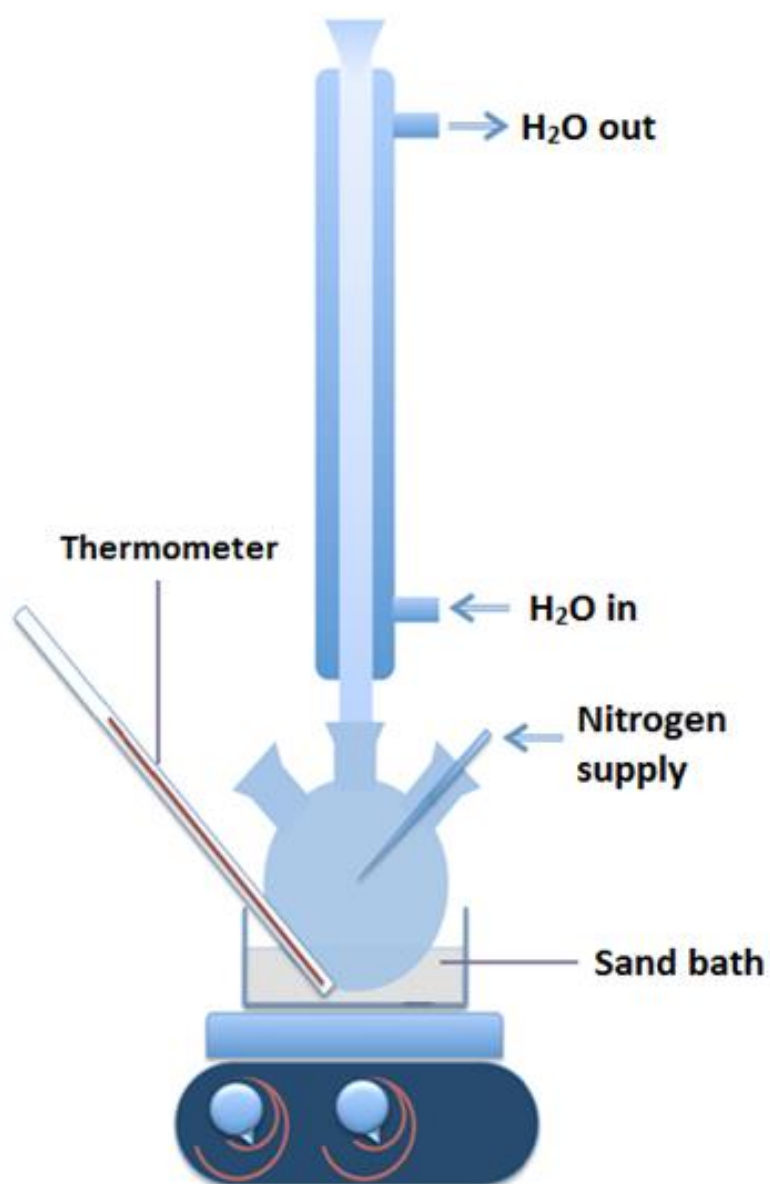
Figure 17: Setup of the reaction vessel for the synthesis of nanocubes. A thermometer was used to measure the temperature of the sand bath.[16]

3.1.1 Synthesis of Magnetic, Decanoic Acid Coated Fe_3O_4 Nanocubes

In a three neck reaction vessel with a reflux condenser as shown in Figure 17, 0.5188 g decanoic acid (3 mmol) and 0.3529 g iron (III) acetylacetonate (1 mmol) was added and mixed. Then, the organic solvent, 25 mL of dibenzyl ether was added. The vessel was set up in a sand bath with a constant nitrogen flow and was sealed to ensure that the system was closed. The reaction mixture was heated to 200 ˚C at a steady heating rate of 5-6 ˚C/min with a stir bar inside the solution to ensure homogeneous mixing of the reagents. During this process, the initial clear orange color of the solution gradually changed to deep red. The solution was maintained at 200 ˚C ± 10 ˚C for 2 hours. The reaction mixture was continued to be heated at the same heating rate of 5-6 ˚C/min until it reached approximately 300 ˚C. The solution was then refluxed at this temperature for an hour which caused it to eventually turn brownish black in color. After this, the heating source was removed and the reaction mixture was allowed to cool to room temperature overnight. FTIR samples were taken 10 minutes after the start of the reaction and also after the reaction was complete.

3.1.2 Washing the Synthesized Nanocubes and Redispersing in Different Solvent Systems

Hexane:acetone (1:1) solution was used for washing the nanocubes. The black reaction mixture was separated into small glass vials and then further transferred to Eppendorf ® Microcentrifuge tubes and washed in batches of four tubes. The following washing protocol was followed for all samples:

The glass vial containing the stock solution was sonicated at first for 5 minutes. Four 1.5 mL Eppendorf ® Microcentrifuge tubes of 50 μL stock solution were prepared. The tubes were filled up to the 1.5mL mark with hexane:acetone (1:1) for washing. The tubes were then sonicated for 5 minutes or until a homogeneous solution of the nanocubes are obtained. They were then centrifuged at 8000 rpm/min for 5 min, after which the clear solution, which is the supernatant liquid was discarded from the top leaving behind small pellets of Fe_3O_4 nanocubes in the bottom of the tubes. The tubes were then refilled up to the 1.5 mL mark and the same procedure of sonication and centrifugation were repeated three more times (a total of four times) to obtain washed nanocubes.

After the supernatant was discarded following the last wash, the samples were then allowed to dry by keeping the tube caps open overnight. Finally, the particles were dispersed in different ratios of chloroform:methanol dispersing agents and also a control dispersing agent of pure chloroform. Different ratios of chloroform:methanol were used as the dispersing agents: 1:4, 1:3, 1:2, 1:1, 2:1, 3:1, 4:1 and pure chloroform was used as a control.

3.2 Confirmation of Magnetic Particles

The presence of magnetic nanocubes can be confirmed with the help of a neodymium magnet. When a small neodymium magnet is placed near a solution of iron oxide nanocubes, the particles are seen to be attracted towards the magnet thus confirming their magnetic nature as shown in Figure 18.
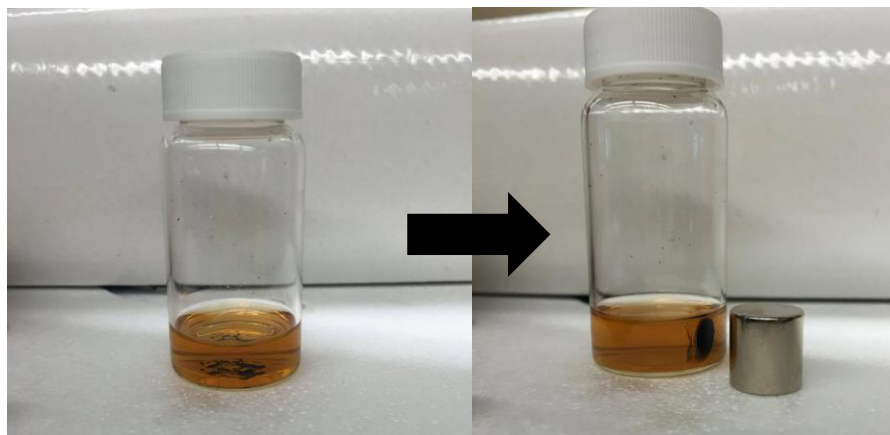
Figure 18: Presence of neodymium magnet near the vial shows attraction of nanoparticles to the magnet.

3.3 Sample Preparation by Drop Casting

3 μL of nanocube solution dispersed in each ratio of chloroform: methanol and pure chloroform were drop casted onto carbon coated TEM grids using a micropipette. The grids were allowed to dry and TEM images were obtained for each ratio of the drop casted samples.

3.4 Sample Preparation Using the Langmuir Trough
3.4.1 Cleaning the Langmuir Trough before Sample Preparation

As mentioned before, since dust particles can interfere with the formation of uniform monolayers at the air-water interface of the Langmuir trough, the trough was intensively cleaned several times before the preparation of samples using deionized (DI) water followed by chloroform. In addition, the nanocube

solutions were also washed thoroughly with hexane: acetone 1:1 ratio to remove residual reagents. The Langmuir trough is first filled with Milli-Q water and a Wilhelmy plate was placed on the electrobalance to measure the surface pressure of water in the trough. Vacuum suctioning was then performed to clean the trough and water surface.

The NIMA software program attached to the Langmuir-Blodgett trough was operated to set the barrier speed at 25 cm^2/min. After setting the pressure to zero, the barriers were allowed to compress. The compression of the barriers generated the surface pressure vs. area isotherm. From the isotherm, if the pressure was seen to drop below -0.2 mN/m, the barriers were stopped and the vacuum was applied to clean the surface of the water again. The lowest surface area the Langmuir trough can reach is 78 cm^2 and at this area, the vacuum set-up was used one last time to clean the surface of the water.

3.4.2 Sample Preparation Using the Langmuir-Schaefer Technique

After the Langmuir trough is carefully cleaned, the barriers were fully opened. For each ratio of the dispersing agent, 250 μL of nanocube solution was spread on the water surface using a micro syringe at room temperature. Then the particles were allowed to stabilize for approximately 5 minutes after which the barriers were allowed to compress with a very slow compression rate of 20 mm^2/min as illustrated in Figure 19. The compression generates an isotherm which can be analyzed to study the two-dimensional phase changes. Isotherms

generated from the sample preparation of each ratio were studied. As the barriers are compressed, the nanocubes are allowed to come close to each other which leads to the packing of the particles into a thin film. After compression the particles were again allowed to stabilize before being transferred onto the substrate.
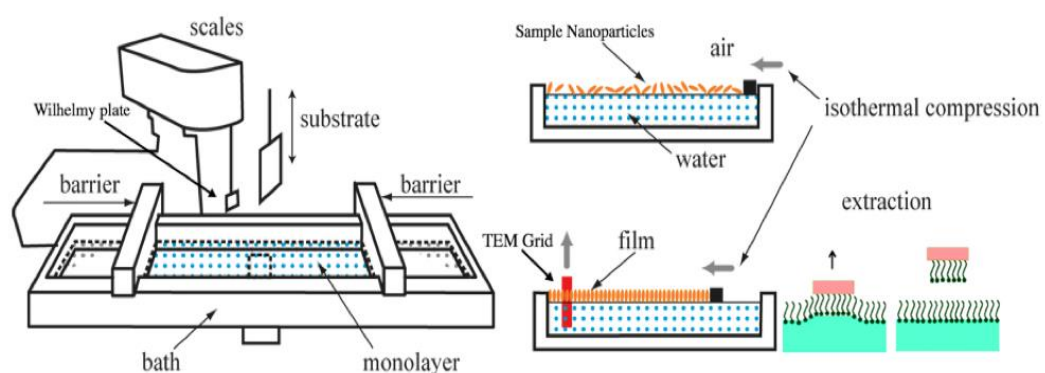

Figure 19: Diagram showing the compression of barriers to allow packing of the nanocubes. The packed layer is then transferred onto a TEM grid using a horizontal extraction technique (LS).[24-26]

A carbon TEM grid was very carefully placed on the surface of the nanocubes so that the grid is parallel to the water surface ensuring that the carbon coated side of the grid was facing down. After letting the grid sit on the water surface for a further 5 minutes, the TEM grid was carefully extracted from the surface of the water in a horizontal motion. The grid was then allowed to air dry so that when the solvent evaporates, a thin film of the nanocubes were left behind on the surface. TEM analysis of the grids for each ratio were analyzed to

understand the behavior and morphology of the nanocubes dispersed in different

ratios of the mixed solvent system.

3.5 Characterization Using TEM to Measure the Nanocube Size Distribution

The samples obtained from the different ratios of the mixed solvent

system of chloroform and methanol, along with the single solvent system of pure

chloroform prepared using drop casting and Langmuir-Schaefer technique were

characterized using TEM. Using a software called ImageJ, the size of particles of

a sample in pure chloroform was analyzed to obtain the size distribution of
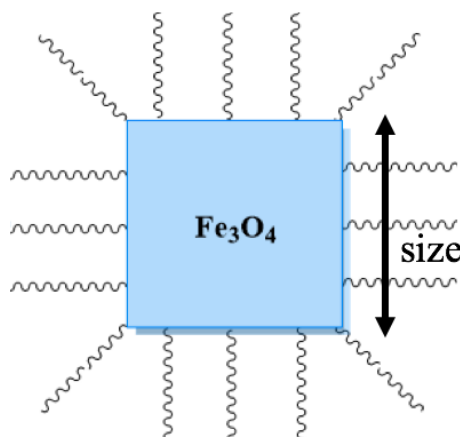
particles.

Figure 20: Measuring the size of a nanocube.

3.6 Characterization Using FTIR to Study Bond Formation and Dissociation

FTIR spectra were obtained using the Bruker-Alpha FTIR to understand

and study the dissociation of existing bonds and formation of new bonds. A

sample of the reaction mixture was taken at about 10 minutes after the reaction started. A second sample was taken from the solution after the reaction was complete and the spectra of the two samples were obtained using FTIR. In addition, the spectra of pure dibenzyl ether and decanoic acid were also measured. To obtain accurate spectra, 32 scans of each sample were carried out and the peaks in the wide range of 750 cm^{-1} to 4000 cm^{-1} were analyzed.

4. RESULTS AND DISCUSSION

4.1 Identification of the Synthesized Fe_3O_4 Nanocubes

The synthesis of Fe_3O_4 nanocubes produced particles with a substantial yield. In solution, the particles could be seen to have a powdery appearance. The decanoic acid surfactant layer allowed the nanocubes to stabilize in solution and hence allowed dispersion of the cubes in mixed solvent systems of chloroform and methanol which have differing polarities, as well as pure chloroform which is slightly polar. However, not all ratios of the chloroform:methanol dispersing agents were favored and it was seen that the nanocubes preferred a higher volume of chloroform than methanol as will be discussed further in the following sections.

As was discussed previously, the synthesized Fe_3O_4 nanocubes were seen to be attracted to a small neodymium magnet as it was brought close to a vial containing some particles. This observation could be used to confirm that the synthesized nanocubes were indeed magnetic. In order to verify the formation of Fe_3O_4 nanocubes, different characterization techniques including FTIR spectroscopy and TEM analysis were carried out, the results of which are summarized and discussed as follows.

4.1.1 FTIR Analysis of the Synthesized Nanocubes

FTIR spectroscopy can provide a good insight into the bonds formed and dissociated as a reaction progresses over time.[37] Figure 21 shows the FTIR spectra of pure decanoic acid. In decanoic acid, there are two significant peaks which are not in the fingerprint region. The first peak is a singlet at 1716 cm^{-1} due to the carbonyl COO$^-$ bond present in the acid and the other is a broad peak due to C-H stretching at approximately 2900 cm^{-1}.
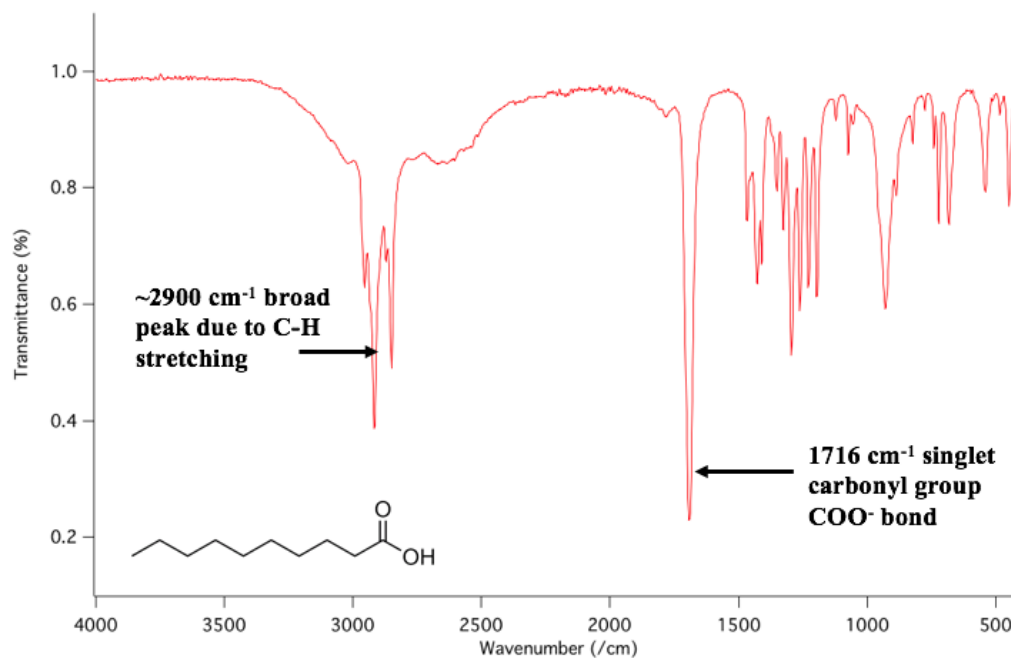

Figure 21: FTIR spectra of pure decanoic acid shows two significant peaks: one is a singlet due to COO$^-$ bond and the other is a broad peak due to C-H stretching.
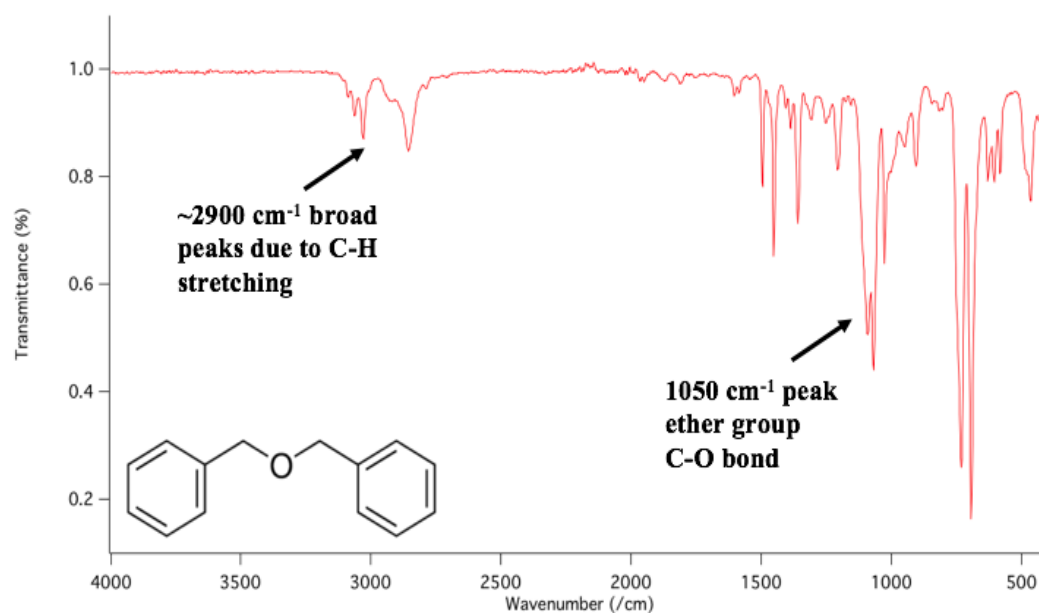
46

Figure 22: FTIR spectra of pure dibenzyl ether shows two significant peaks: one is a strong peak due to C-O ether bond and the other broad peaks are due to C-H stretching.

Similarly, as shown above, Figure 22 shows the FTIR spectra of pure dibenzyl ether. This spectrum also shows two significant peaks. The first peak is a strong peak due to C-O ether bond at 1050 cm^{-1} and the other broad peaks are due to C-H stretching at approximately the 2900-3000 cm^{-1} region. Figure 23 shows the spectra of a sample of the reaction mixture after reaction was complete. On the spectrum, iron-oxygen Fe-O bond formation is observed which can be seen from the peak at 579 cm^{-1} due to the formation of Fe_3O_4 nanocubes. This peak was not previously present in both the decanoic acid and the dibenzyl ether spectra. In addition to that, the peak at 1716 cm^{-1} is due to carbonyl group disappearance. This is because decanoic acid stabilizes the synthesized nanocubes

47

and the strong signal is replaced by the symmetric and asymmetric stretching vibrations of the carboxylate group.

In addition to these peaks, the peak at approximately 1600 cm^{-1} seen in the spectra corresponds to a C=O stretch for iron carboxylate salts.[40] A reason for this might be due to residual iron acetylacetonate. The small peaks in the range of 2800-3300 cm^{-1} in the C-H bond region correspond to alkyl groups in the decanoic acid.
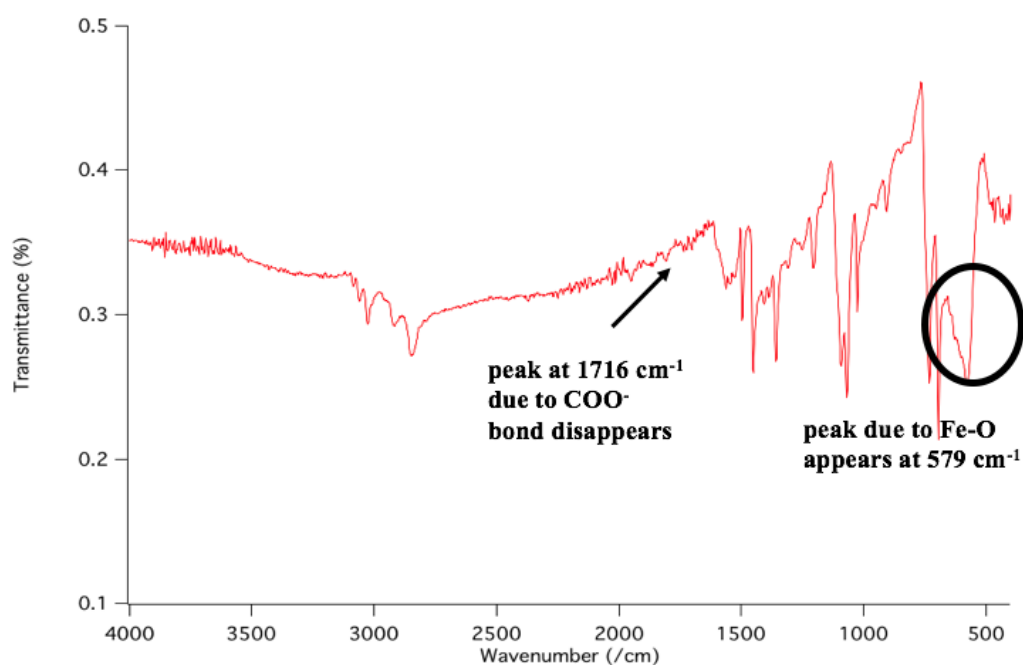

Figure 23: FTIR spectra of a pellet of dry Fe$_3$O$_4$ nanocubes show the formation of Fe-O bond and the disappearance of COO$^-$ bond.

Therefore, from the spectrum of the synthesized nanocubes it can be confirmed that the decanoic acid is chemically bound to the surface of the nanocubes.

4.2 Analysis of the Assembly of Fe₃O₄ Nanocubes

The TEM micrographs of the samples prepared using the two methods, drop casting and Langmuir-Schaefer technique were analyzed to study the assembly of the nanocubes dispersed in the varying chloroform and methanol ratios as they were deposited on carbon TEM grids. In the TEM images listed below, the image on the left will always correspond to an image with a lower magnification on the grid and the image on the right will always correspond to an image with a higher magnification.

4.2.1 TEM Analysis of Samples Dispersed in Pure Chloroform

In Figure 24, the TEM image of a sample dispersed in pure chloroform is shown that is prepared using drop casting. For particles dispersed in pure chloroform, specks of particles were spread throughout the TEM grids. In addition, thinner layers were seen in different regions on the grid which means that the nanocubes prefer chloroform more.
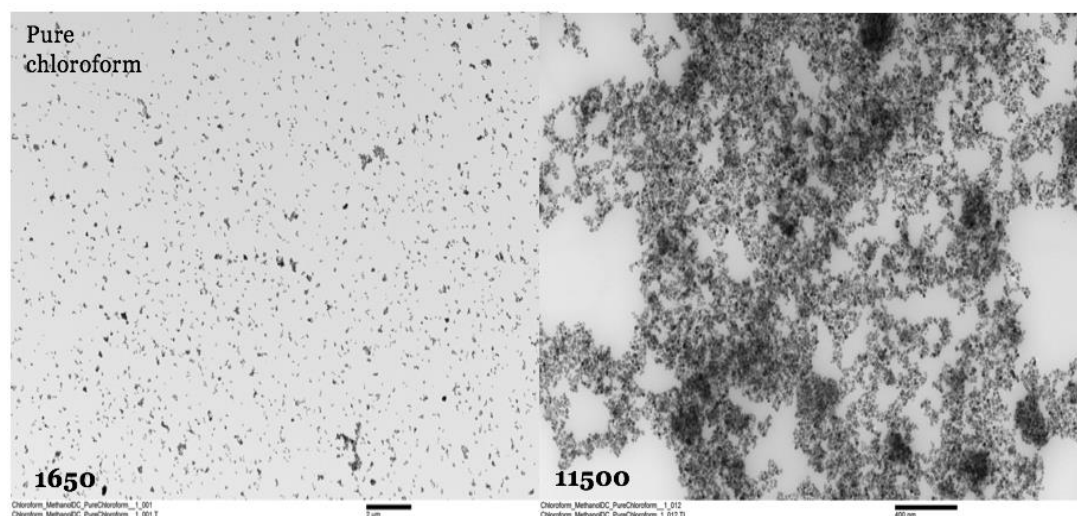
Figure 24: TEM images of nanocubes dispersed in pure chloroform. The image on the left was recorded at a magnification of 1650 and the one on the right was recorded at a magnification of 11500. This sample also has specks of the nanocubes throughout larger areas of the TEM grids.

When samples prepared using the LS technique were studied for the nanocubes dispersed in pure chloroform, thinner layers of the nanocubes were also observed. Even though the layers observed were thin, gaps were observed between the cubes which meant that uniform packing was not achieved over large areas. However, from the surface morphology of the nanocubes, it can be seen from the figure below that pure chloroform is a good dispersing agent on its own as it prevents the formation of large aggregates of the particles.
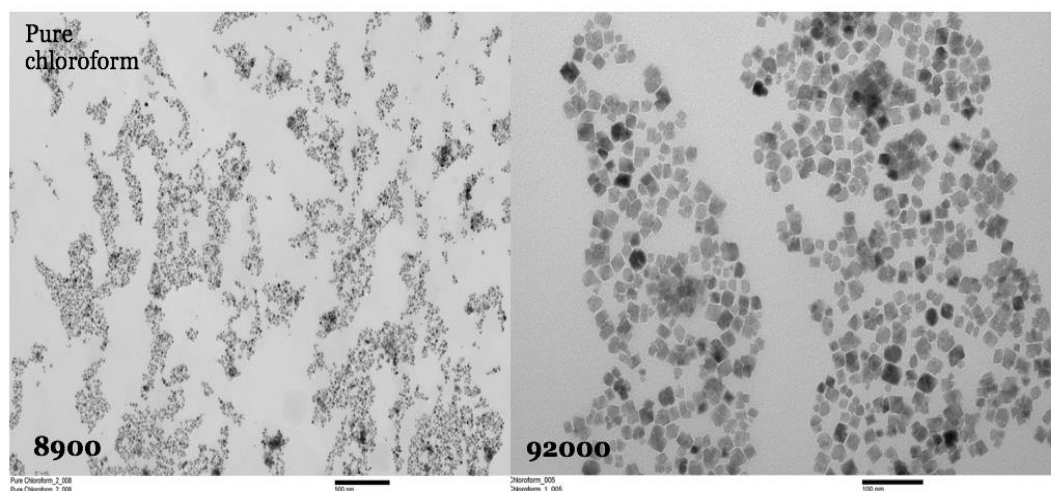
Figure 25: TEM images of nanocubes dispersed in pure chloroform showed particles packed in very thin layers throughout the grids. However, gaps showed that packing was not uniform.

4.2.2 TEM Analysis of Samples Prepared Using Drop Casting for different ratios of Chloroform:Methanol

In Figure 26, TEM images of the nanocubes dispersed in chloroform:methanol 1:4 are shown which were formed by drop casting. All throughout the TEM grid, circular specks of the cubes were observed. This could be the due to the differences in evaporation of the two solvents. The boiling point of chloroform is 61.2 °C while the boiling point of methanol is 64.7 °C. This means that chloroform evaporates faster from the solvent mixture. As chloroform evaporates, the particles prefer to be in chloroform and hence come together as the chloroform evaporates leaving behind circular specks on the grid. Finally, the methanol dries out and forms the specific patterns.
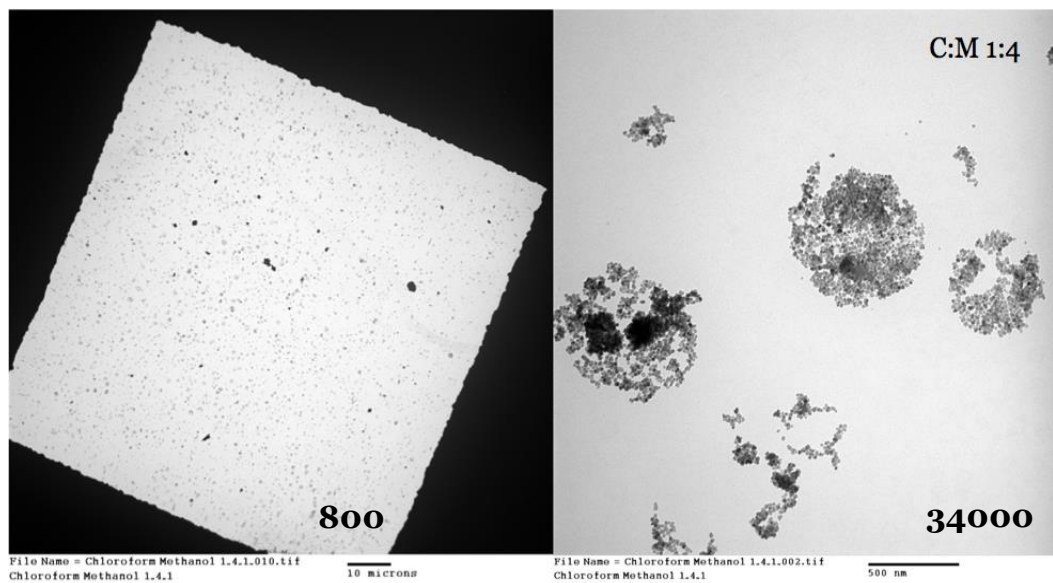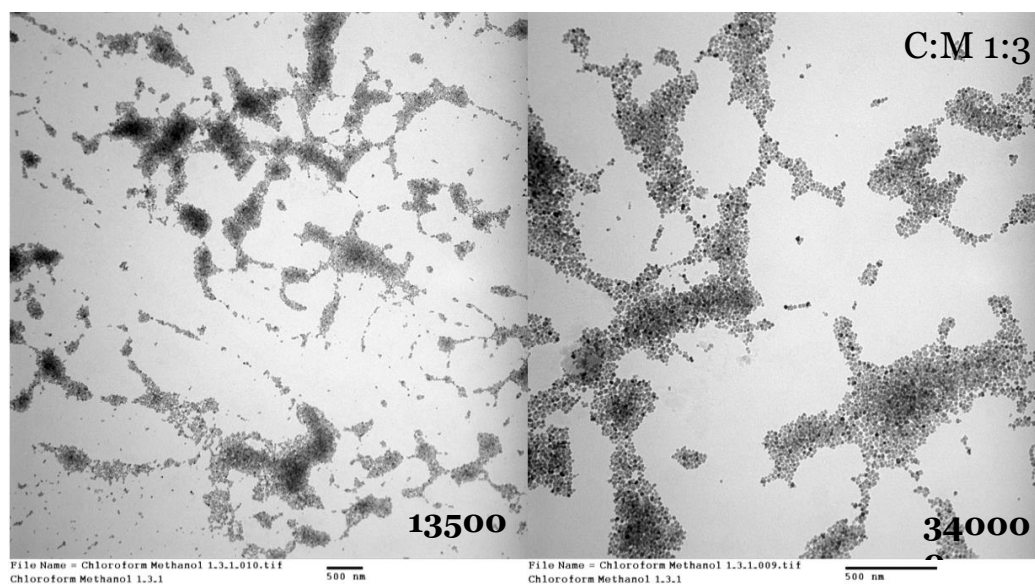
Figure 26: TEM images of nanocubes dispersed in chloroform:methanol 1:4. The image on the left was recorded at a magnification of 800 and the one on the right was recorded at a magnification of 34000. This sample shows interesting drying where circular assemblies of the iron oxide cubes were formed.

Similarly for Figure 27, interesting drying mechanisms were also observed for nanocubes in chloroform:methanol 1:3. In this sample as well, as chloroform has a lower volume ratio than methanol, the particles are seen to coalesce close together as they prefer to be in chloroform. Hence regions with darker, more aggregated areas are seen which were surrounded by lighter, thinner layers of nanocubes as the particles dried in chloroform.

Figure 27: TEM images of nanocubes dispersed in chloroform:methanol 1:3. The image on the left was recorded at a magnification of 13500 and the one on the right was recorded at a magnification of 34000. This sample also shows interesting drying where random assemblies of the iron oxide cubes were formed.

Previous research in our group showed that hexane, being a non-polar solvent was not a suitable dispersing agent for nanospheres coated with octanoic acid.[17] Apart from hexane, a mixed solvent system of octane and toluene were also used to disperse the octanoic acid coated particles but with almost no success as the particles did not favor the non-polar nature of the solvents. For this reason, a different mixed solvent system of chloroform and methanol was studied with differing polarities, as methanol is polar and chloroform is slightly polar.[17] According to research conducted by Orbulescu *et al.*, for monolayers prepared using the Langmuir trough, the solvent choice was extremely important as it dictates the interaction of the particles during the deposition at the air-water interface.[34]
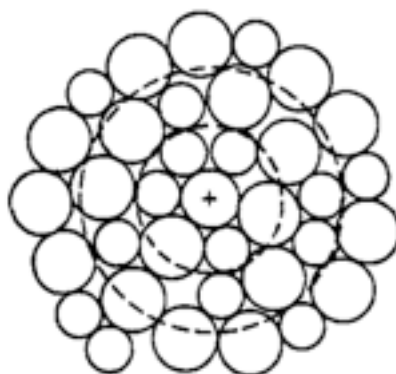
Figure 28: Diagram of a schematic cation dispersed in two different solvents denoted by the two different sphere sizes surrounding the cation with molar volume ratio of 1:2.[35]

A mixture of chloroform:methanol is hypothesized to behave in a very similar fashion as shown in Figure 28, where the ions, or in this case the nanocubes, prefer one type of solvent molecule over the other in the first layer surrounding it but as the number of layers increases, the preference diminishes.[35] Therefore, due to the stability provided by the two different solvent molecules, the nanocubes are able to disperse homogeneously in solution without the formation of aggregates.
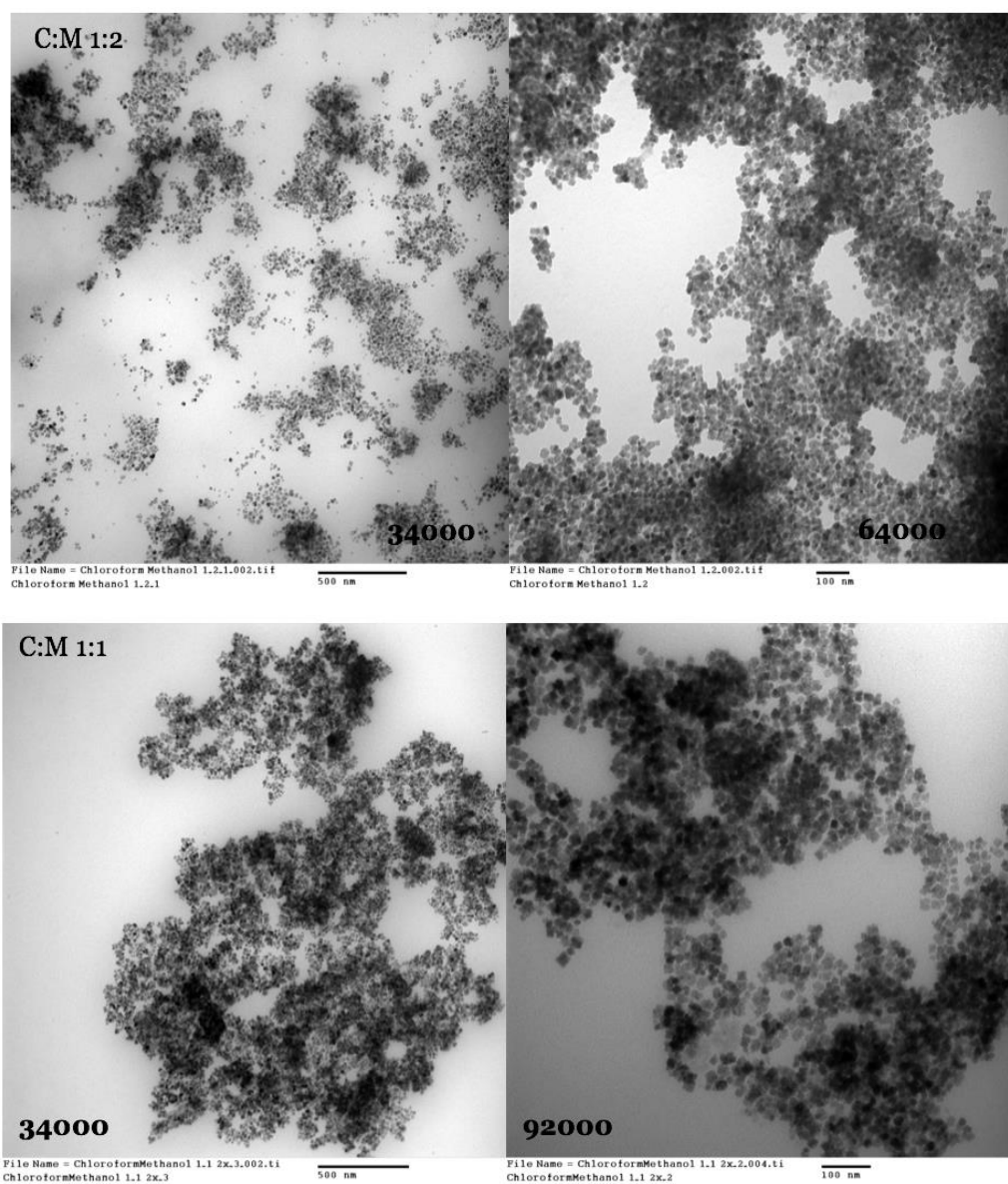
Figure 29: TEM images of nanocubes dispersed in chloroform:methanol 1:2 and 1:1. This sample showed aggregation of nanocubes with large gaps in packing.

For the TEM images of the samples from volume ratios of chloroform:methanol 1:2 and 1:1, highly aggregated areas of the nanocubes were observed with large gaps thus no uniform packing as shown in Figure 29.

Nanocubes dispersed in chloroform:methanol 2:1, 3:1 and 4:1 showed highly aggregated particles with large gaps between the particles as can be seen in the next figure. This means that these ratios were not suitable for the formation of uniform monolayers of the nanocubes.
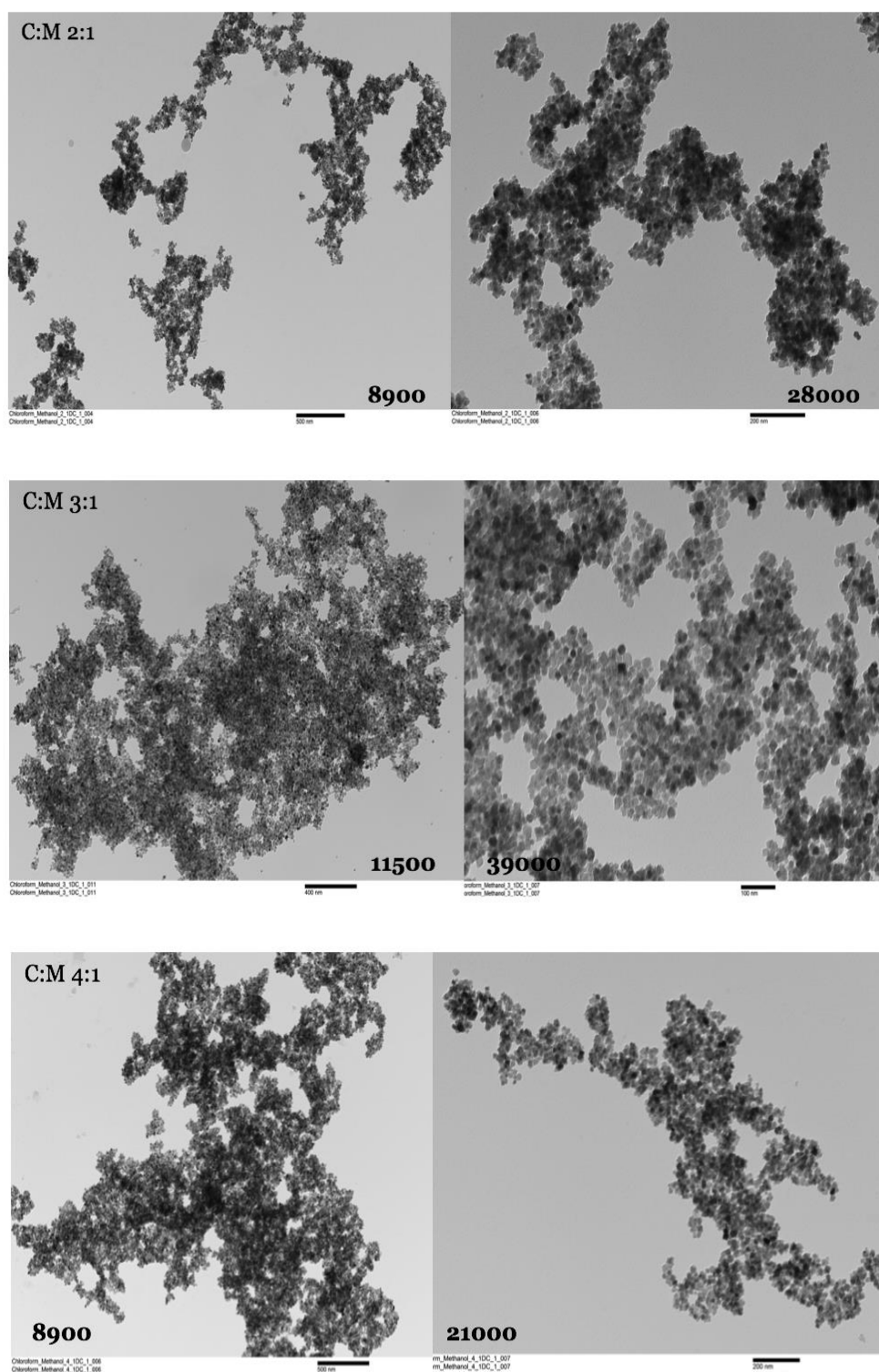
Figure 30: TEM images of nanocubes dispersed in chloroform:methanol 2:1, 3:1 and 4:1 showed highly aggregated particles.

4.2.3 TEM Analysis of Samples Prepared Using Langmuir-Schafer technique for different ratios of Chloroform:Methanol

As was seen in the drop casting samples, iron oxide nanocubes deposition using Langmuir-Schaefer technique for the ratio of chloroform:methanol 1:4 and 1:3 showed interesting drying patterns as well. The particles form patterns due to the well-known "coffee ring effect" where the pattern is obtained after a liquid evaporates and leaves behind a ring of previously dissolved solid.[36] As the volume ratio of chloroform was lower than methanol in the two samples, small amounts of the nanocubes were left behind as it dried.

However, zooming into the individual specks around the ring showed ordered and crystalline packing with some gaps between the particles. Even though the gaps were small, particles were seen to form thin, even monolayers with little agglomeration. The TEM images for 1:4 and 1:3 are shown in Figure 31 as follows.
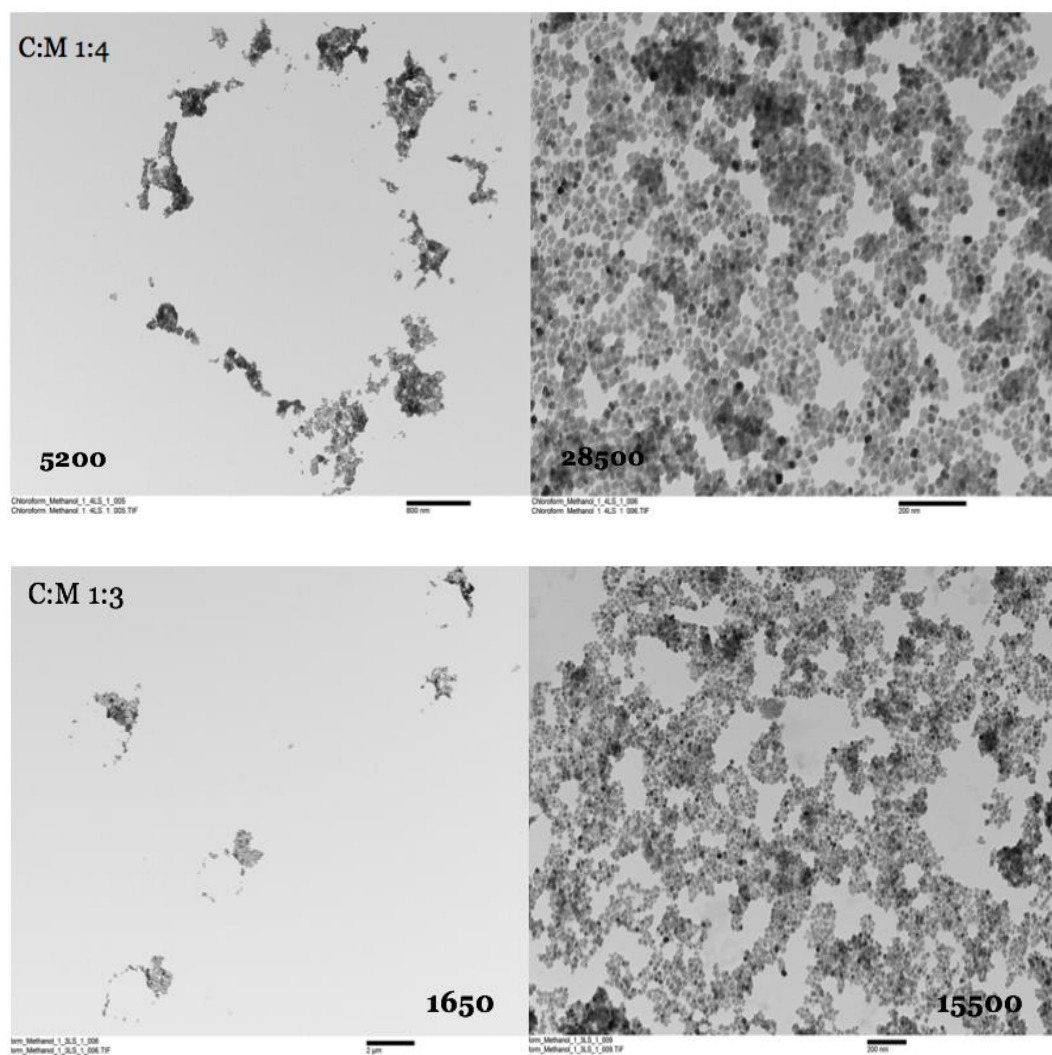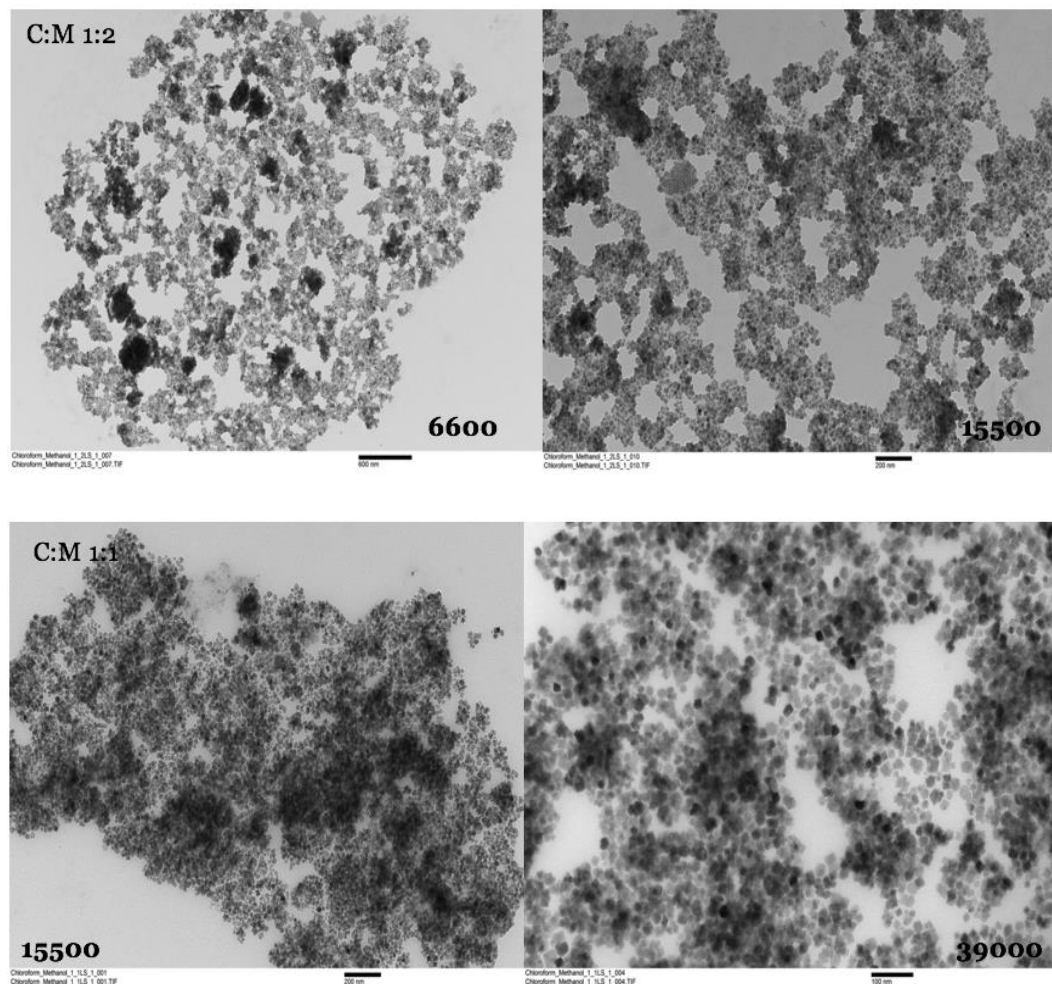
Figure 31: TEM images of nanocubes dispersed in chloroform:methanol 1:4 and 1:3 prepared using LS technique showed particles undergoing "coffee ring effect".

From the TEM images in Figure 32, for the LS technique for the ratios of chloroform:methanol 1:2 and 1:1, the nanocubes were seen to be packed over large areas of the TEM grid. However, even though the particles packed in thinner layers, gaps were present throughout the layers of particles. Some aggregation of the particles could also be seen but this could be due to the formation of

multilayers as the barriers of the Langmuir trough compressed leading to the

stacking of the nanocube layers.

Figure 32: TEM images of nanocubes dispersed in chloroform:methanol 1:2 and 1:1 prepared using LS technique showed particles packed over larger areas but with gaps.

Samples prepared using the LS of 2:1 ratio were not ideal as large

aggregated areas were observed all throughout the TEM grid [Figure 33].
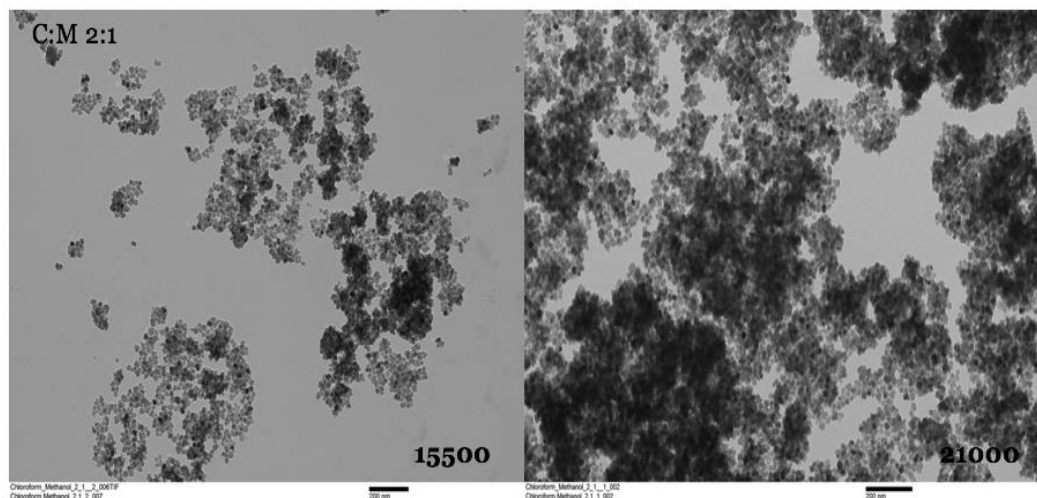
Figure 33: TEM images of nanocubes dispersed in chloroform:methanol 2:1 showed particles that were highly aggregated.

In addition, samples dispersed in 4:1 chloroform:methanol showed

packing over large areas that were thin but also contained gaps between the layers

[Figure 34]. One reason for this continued trend of the samples might be that

concentration of the nanocubes in solution were not enough for the formation of

tightly packed crystalline monolayers. Low concentration of particles hinders the

formation of uniformly packed layers thus resulting in the gaps as the Langmuir

barriers are compressed.
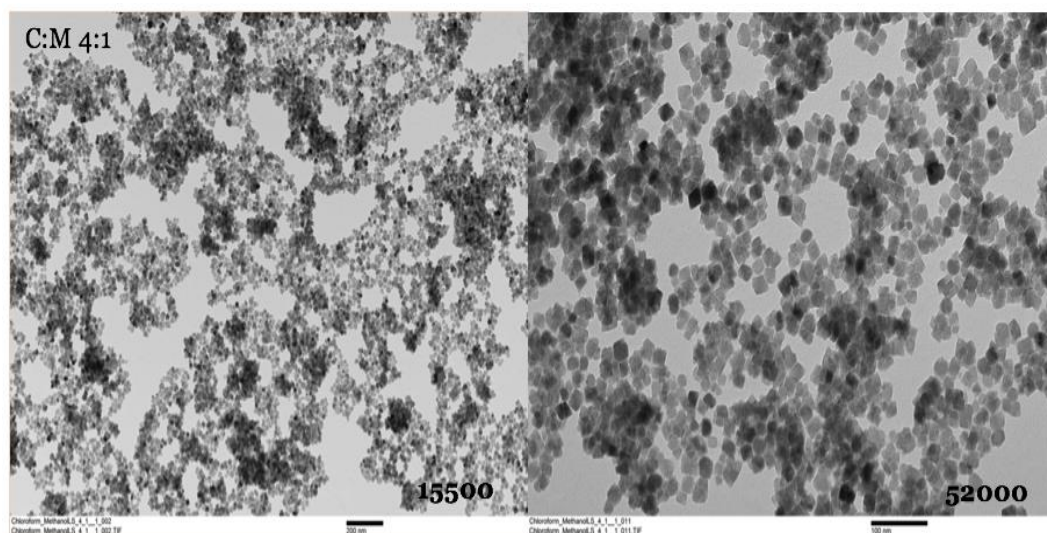
Figure 34: TEM images of nanocubes dispersed in chloroform:methanol 4:1 showed particles that were non-uniformly packed over large areas.

Finally, in Figure 35, TEM images obtained for nanocubes dispersed in chloroform:methanol 3:1 were seen to form crystalline, well-packed monolayers over the majority of the surface on the substrate. The images show very little gaps between the packed layers. The image on the right that is obtained at a higher magnification of 39000 showed little aggregation of particles over the large area. From the image on the left, which was obtained at a magnification of 8900, long and thin areas are seen which are much darker. This corresponds to the formation of multilayers as particles packed close together during the Langmuir-Schaefer technique. It was likely that the barriers might have been compressed too much which caused the monolayer to collapse, leading to the formation of multilayers as shown by the darker regions. Therefore, from these images, it can be observed

that chloroform:methanol 3:1 is a suitable dispersing agent for decanoic acid

coated nanocubes due to the formation of well packed areas over large regions.
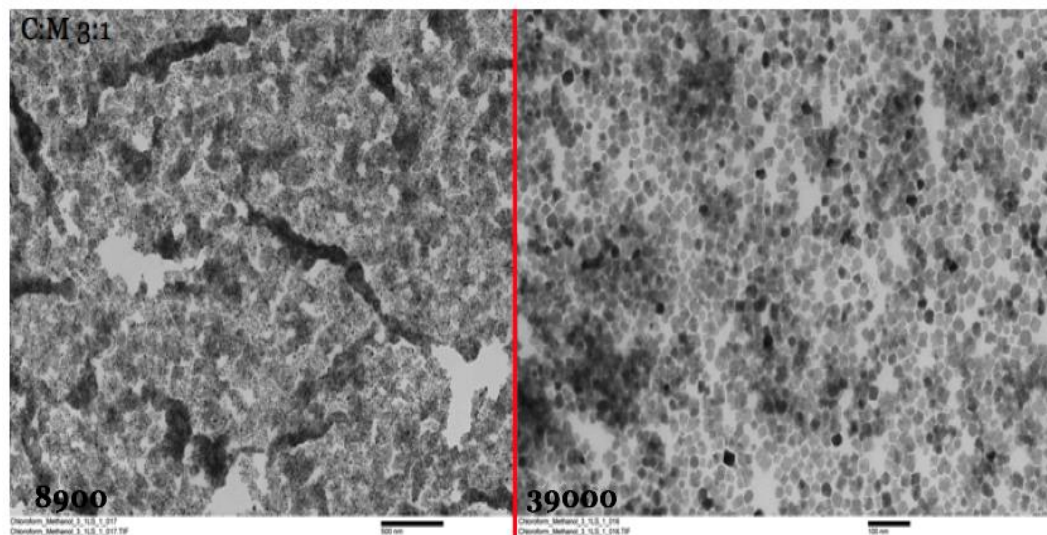
Figure 35: TEM images of nanocubes dispersed in chloroform:methanol 3:1 showed well packed monolayers.

4.2.4 Overview of the TEM Images Obtained From Drop Casting and

Langmuir-Schaefer Technique

Table 2: Summary of TEM images obtained from drop casting and LS for the ratios, 1:4, 1:3, 1:2 and 1:1. The images on the left of each column are of low magnification while the image on the right is of a higher magnification.
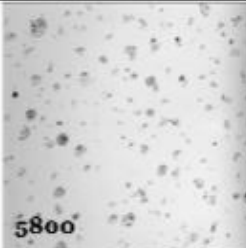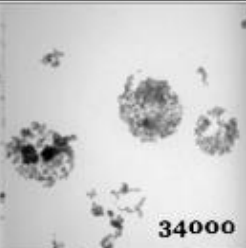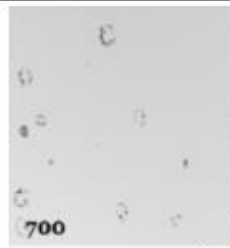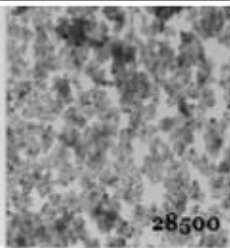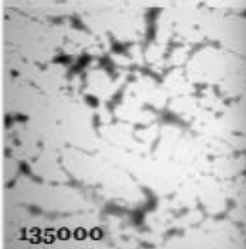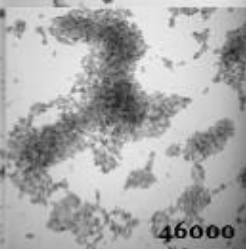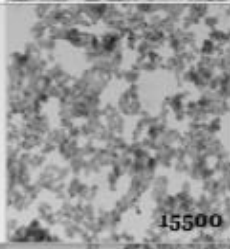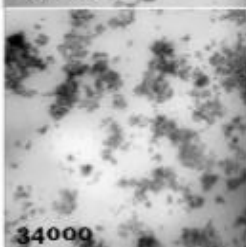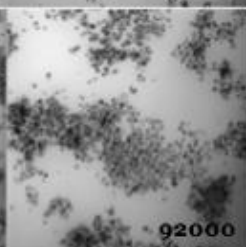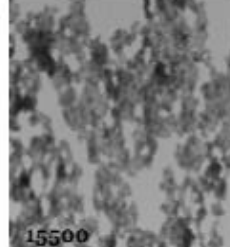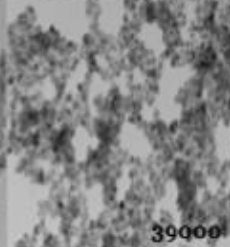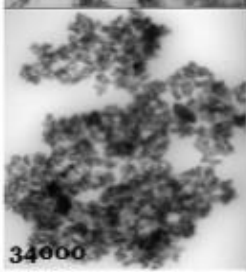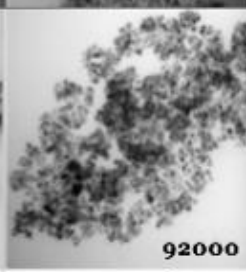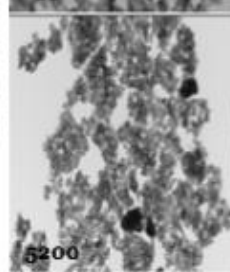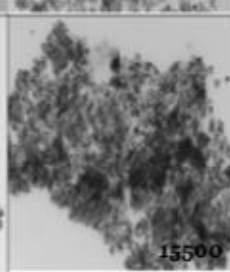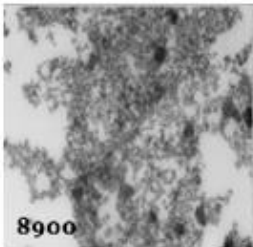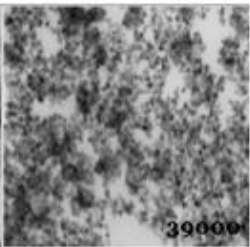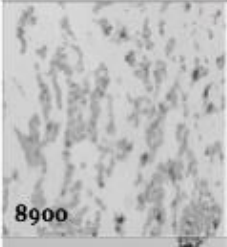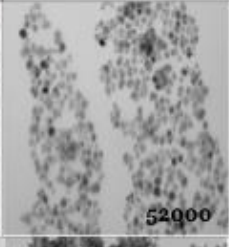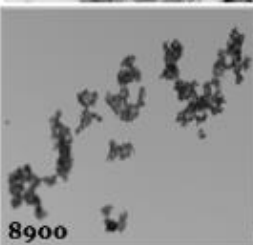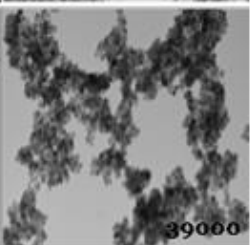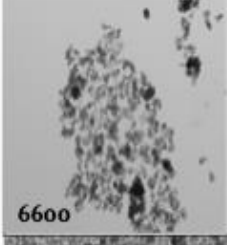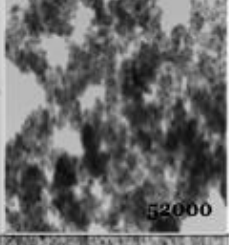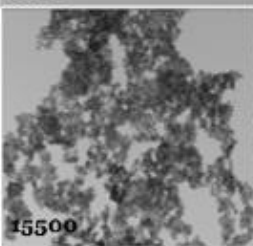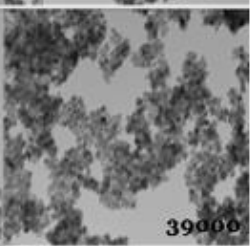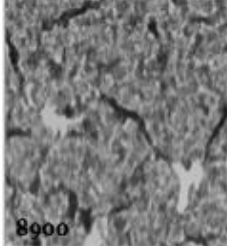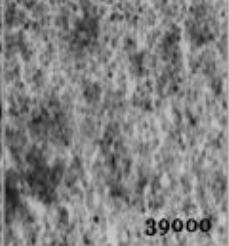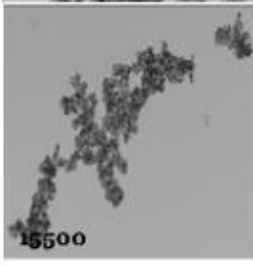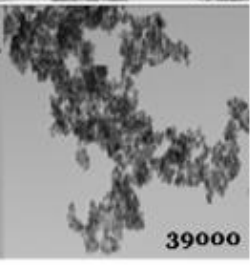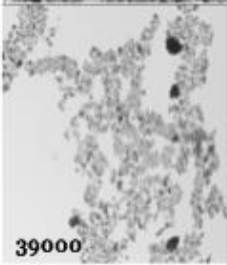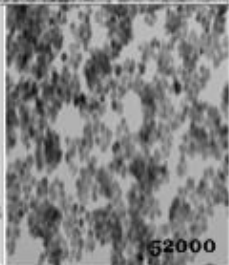
Table 3: Summary of TEM images obtained from drop casting and LS for the ratios, pure chloroform, 2:1, 3:1 and 4:1. The images on the left of each column are of low magnification while the image on the right is of a higher magnification.

4.3 Study of Isotherms Generated from Langmuir-Schaefer Technique

The isotherms generated from the phase transitions during the Langmuir-Schaefer technique can be overlaid to study the packing behavior of the Fe_3O_4 in different ratios of chloroform and methanol.

In order to optimize the amount of the nanocube solution required to obtain a suitable isotherm, different volumes of nanocube solution in chloroform:methanol 1:1 were tried out. Initially 200 μL was used, however as shown in Figure 36, it could be seen that the volume of the nanocube solution was not enough to obtain a suitable isotherm. Hence, 300 μL was used but even then the isotherm did not undergo a phase transition to the solid state. As a result, the concentration of the nanocube solution dispersed in different ratios of chloroform:methanol was doubled. Finally, 235 μL of the nanocube solution dispersed in chloroform:methanol 1:1 was used to perform LS which resulted in much clearer phase transitions. In order to allow the monolayers to reach a 2D solid phase close to the collapse point where crystallinity is highest the optimized volume of nanocube solution for each LS technique was therefore taken to be 250 μL which is slightly greater than 235 μL.
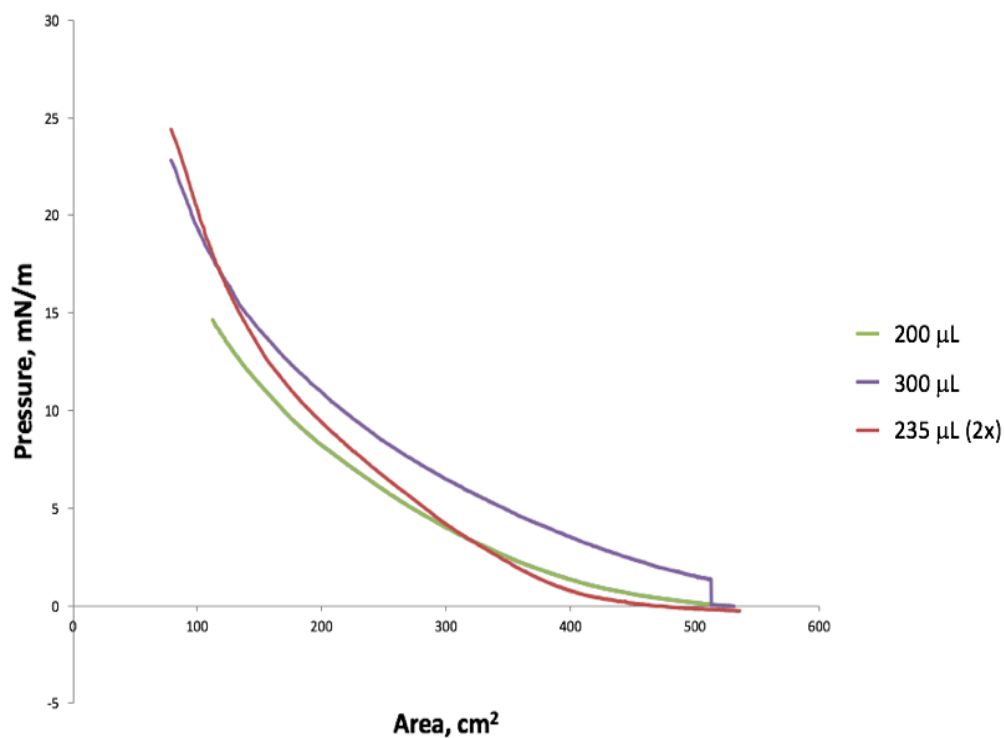
Figure 36: The isotherms of the different trials of nanocubes dispersed in chlorform:methanol 1:1 ratio that were analyzed to determine the optimized volume of 250 μL.

Using a volume of 250 μL of each dispersed nanocube solution in the different ratios, LS technique was performed to obtain monoloyers of nanocubes at the air-water interface which were carefully transferred onto TEM grids after which the isotherms were analyzed. The isotherms obtained from the different ratios were overlaid as shown in Figure 37.
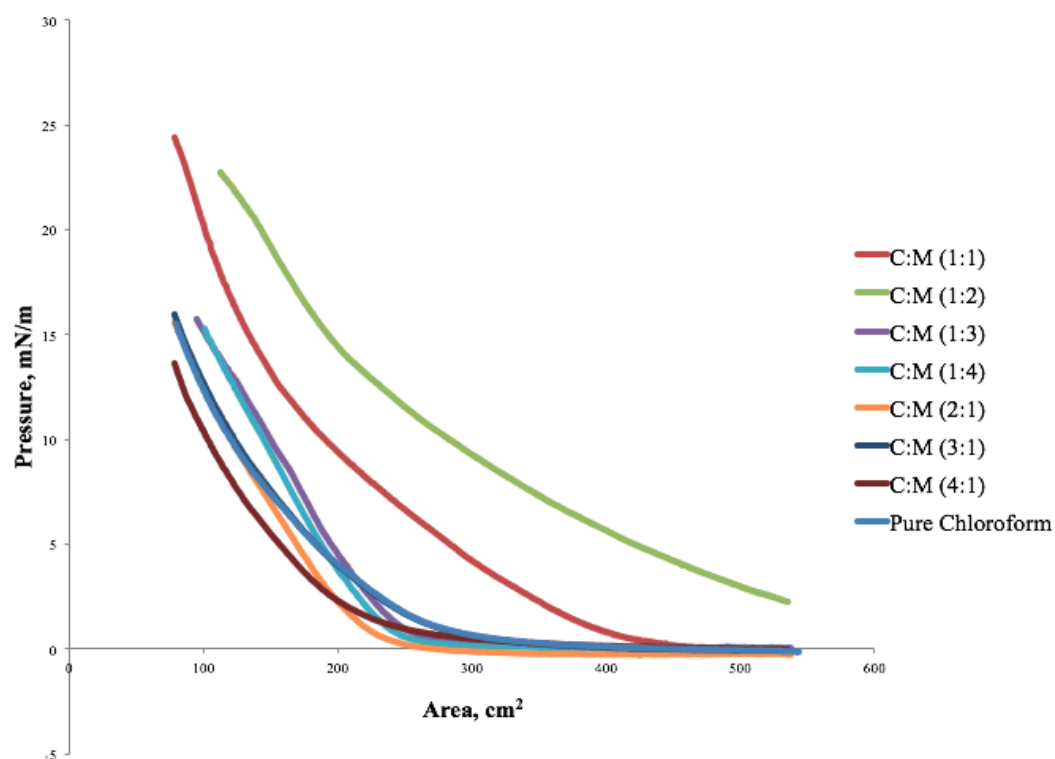
Figure 37: Surface pressure vs. area isotherms for monolayers prepared with various chloroform: methanol ratios.

By comparing the isotherms, it can be seen that when the chloroform ratio is higher than methanol, the slope on the isotherm is steep and quickly transitions to the solid phase. With low or equal volume ratios of chloroform:methanol such as 1:2 and 1:1, the isotherms are quite shallow. According to previous research conducted by Losche et al., in the preparation of depot medroxyprogesterone acetate, or DMPA monolayers, high concentrations of the salt, $CaCl_2$, led to the disappearance of the gas-to-liquid phase change as shown in Figure 38.[33] In our study, the concentration of particles are equal for all ratios of the dispersing agents, hence, this difference in behavior is not quite well understood.
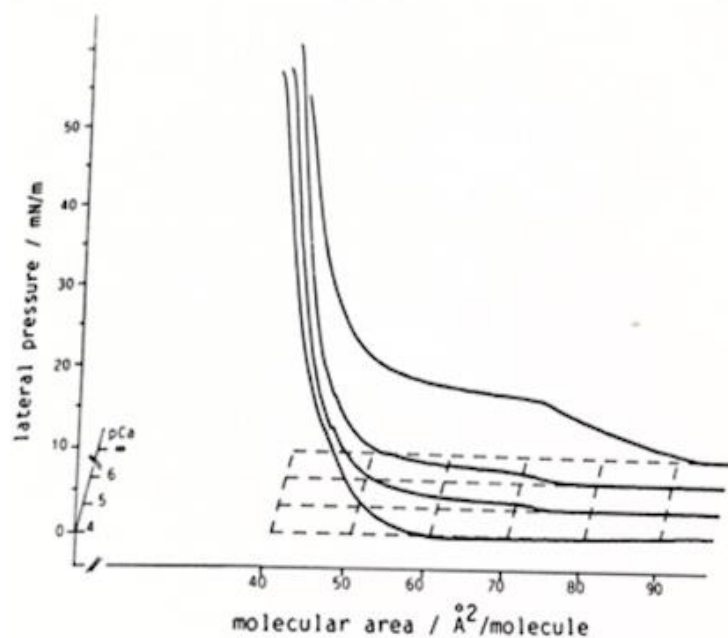
Figure 38: Pressure vs. area isotherms for DMPA monolayers for various $CaCl_2$ concentrations. Higher concentration of the salt causes the disappearance of the gas-to-liquid phase transition.[33]

In addition to salt concentration, temperature also plays a key role in the shape of the isotherm. According to Losche et al., at temperatures below room temperature, that is around 10 °C, the gas-to-liquid phase transition disappears as well shown in Figure 39 below.[33] In our study this factor does not play into effect that much as the surrounding temperature is maintained at a constant.
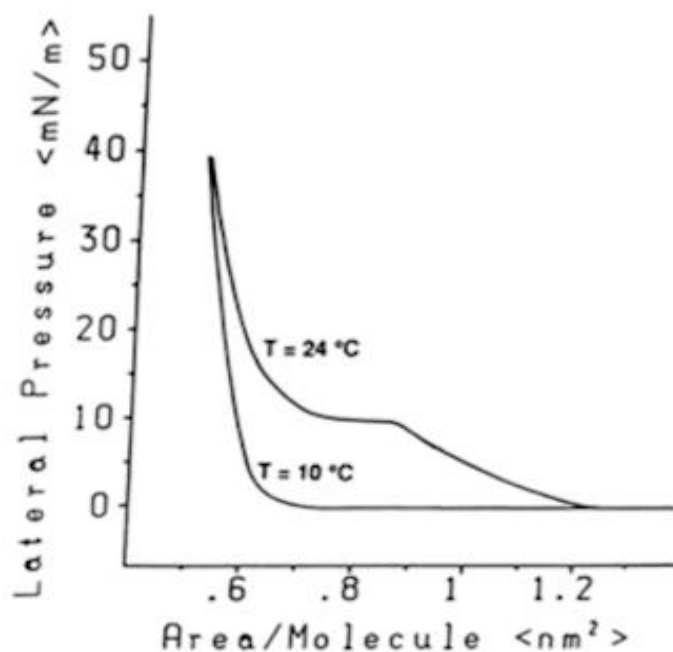
Figure 39: Pressure vs. area isotherms at two different temperatures, 10 °C and 24 °C. Temperatures lower than room temperature causes the disappearance of the gas-to-liquid phase transition.[33]

As shown in Figure 40, slope analysis of the gas-to-solid phase transition is carried out. The slope of a pressure-area isotherm corresponds to the compressibility C of the monolayer. According to the results, the monolayer formed by nanocubes in chloroform:methanol ratio of 1:2 is the least compressible. On the other hand, from the trend in the slope, compressibility is somewhat high for chloroform:methanol 3:1 and pure chloroform and the highest for 4:1. Therefore it can be predicted that higher chloroform volume concentrations, should be able to provide good crystalline packing because they will have highest compressibility. These predictions could be confirmed from the

TEM morphology of 3:1, 4:1 and pure chloroform ratios where good packing of

the nanocubes were observed.
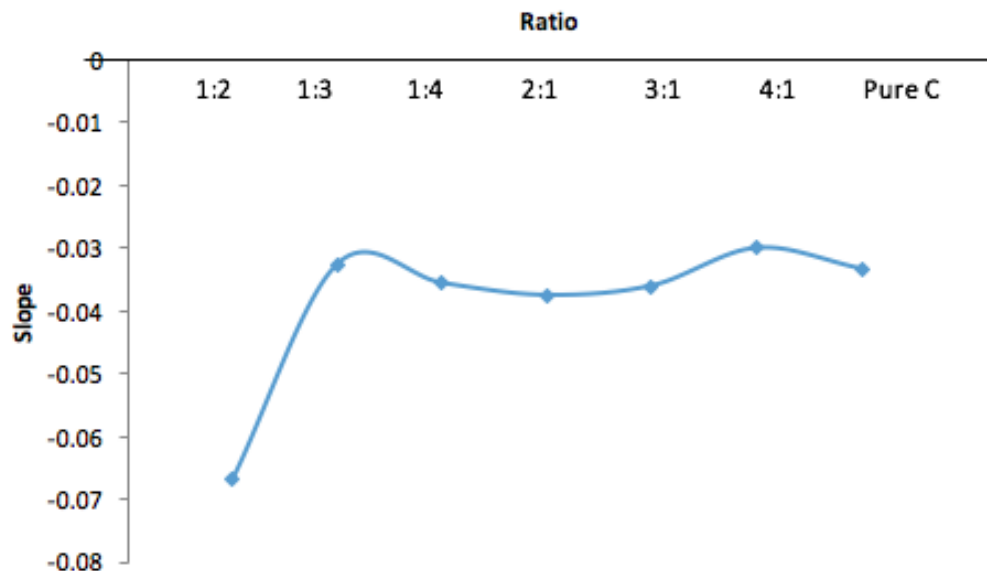
Figure 40: Slope analysis of gas-to-solid transition phase. The isotherm for chloroform:methanol 1:1 does not have a gas-solid transition as shown in Figure 37 above.

4.4 Measurement of Nanocube Size Distribution Using ImageJ

Using the TEM image of a sample of nanocubes dispersed in pure

chloroform, which was prepared using Langmuir-Schaefer technique, the lengths

of particles were measured using ImageJ. This image was chosen because the LS

technique for nanocubes dispersed in pure chloroform produced thin monolayers

of particles which had a good separation and very little aggregation. As shown in

Figure 41 below, the area on the image outlined in red was the region where the

size measurement was carried out. Since a small region of the image was used,

only about 127 nanocubes were measured to plot the size distribution. The size of the nanocubes ranged from 4.039 nm to 25.970 nm. From the distribution, the average size of the nanocubes were determined to be 14.2 ± 4.0 nm.

Average size: 14.2 ± 4.0 nm
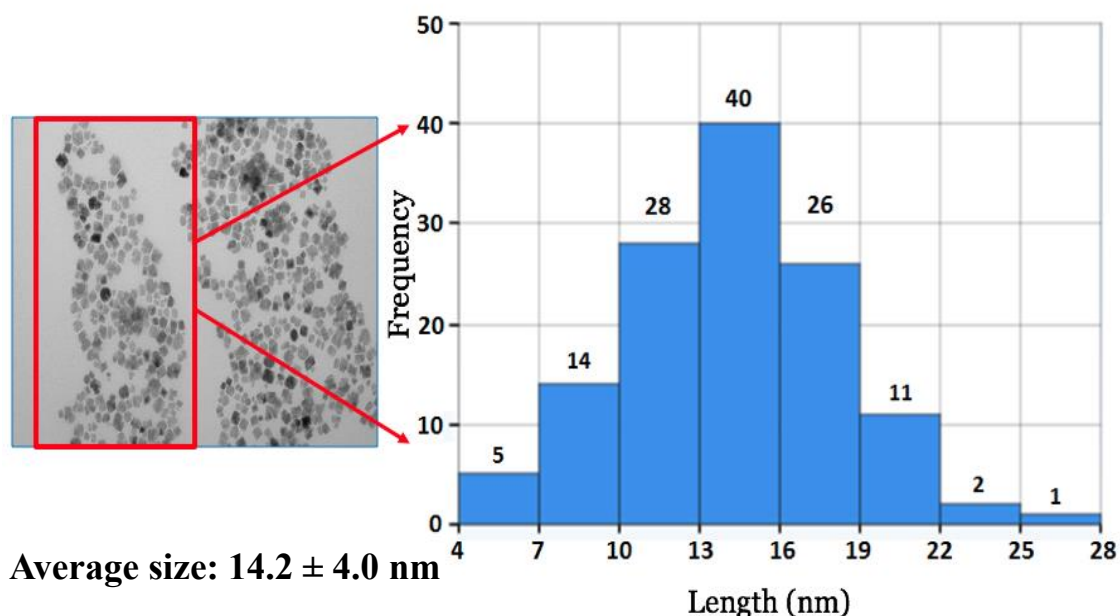
Figure 41: In the above figure, the area outlined in red was the region where the lengths of particles were measured using ImageJ. From this region, the size of about 127 nanocubes were measured and the size distribution was plotted. Using the histogram, the average size of the nanocubes were measured to be 14.2 ± 4.0 nm.

As was mentioned in the introduction, the superparamagnetic limit of iron is approximately 6 nm. Since the average size is about 14.2 nm with a standard deviation of 4 nm, this means that the synthesized nanocubes are quite close to approaching the superparamagnetic state. For iron (III) oxide nanocubes, the superparamagnetic limit is often less than 10 nm which means that the

72

synthesized nanocubes lie somewhere between the ferromagnetic and

superparamagnetic regions.
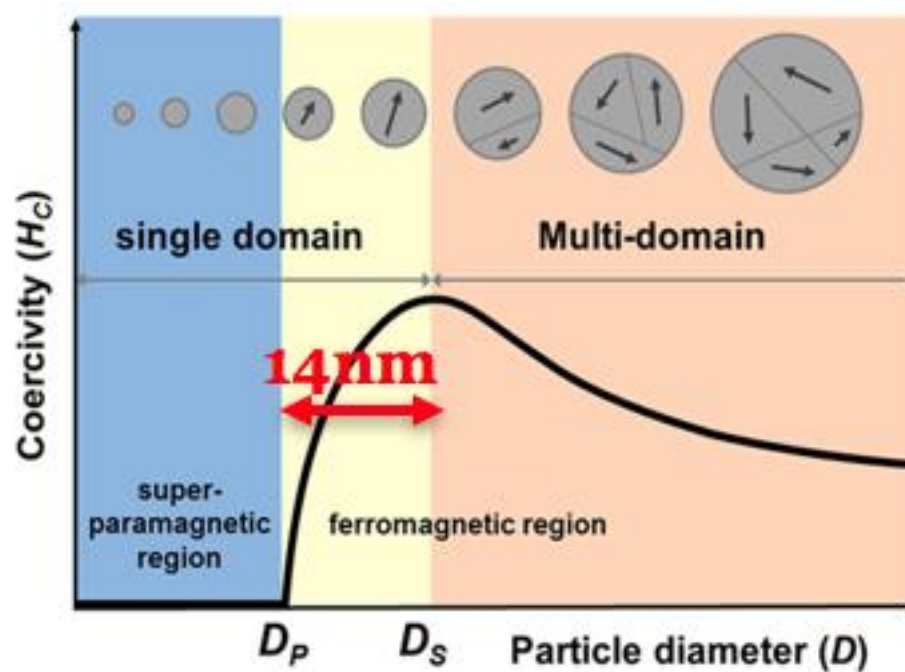
Figure 42: Since the average size of the nanocubes is 14.2 ± 4.0 nm, this means that the cubes lie between the ferromagnetic and superparamagnetic regions.[8]

5. CONCLUSIONS AND FUTURE WORK

Using the thermal decomposition of iron acetylacetonate, magnetic iron (III) oxide nanocubes could be successfully synthesized to obtain particles with a relatively narrow size distribution. The synthesized particles were highly crystalline and could be used to prepare well-packed monolayers by altering the dispersing agent. Since the assembly and characterization is less researched, this study provided an easy approach to the synthesis of magnetic iron (III) oxide which can be used for the formation of monolayers. Study of the assembly of these nanocubes is essential as iron oxide nanoparticles have a great potential in magnetic data storage and in biomedicine.[1]

FTIR spectroscopy could be used to understand the bond formation and disassociation that occurs during synthesis of the iron oxide nanocubes. FTIR can be used to characterize and confirm the presence of decanoic acid coating on these nanocubes. A peak appearance at 579 cm^{-1} confirmed the formation of Fe-O bond in the Fe_3O_4 nanocubes.[37] In addition to that, the peak at 1716 cm^{-1} due to COO^- disappears and at the same time, peaks in the range of 2800-3300 cm^{-1} in the C-H bond region correspond to COO^- bond stretching in the carboxyl group of decanoic acid coating.[40]

Transmission electron microscopy (TEM) was used to obtain information about the shape, size, crystallinity and packing of the decanoic acid coated nanocubes. Using two different techniques, Langmuir-Schaefer and drop casting,

thin films of the synthesized nanocubes were prepared. The nanocube solutions were dispersed in varying ratios of chloroform and methanol ranging from 1:4 to 4:1 by volume along with pure chloroform as the control. TEM analysis showed interesting drying pattern for both drop casted and LS samples of 1:4 and 1:3 volume ratio of chloroform and methanol. For the LS techniques "coffee ring effects" were observed after the samples dried. In addition chloroform:methanol 3:1 provided the best result in assisting the formation of nanocube monolayers. Although pure chloroform samples were useful in preparing thin monolayers, the TEM results confirm that a mixed solvent system of chloroform and methanol worked better than just a single solvent system in the formation of well-packed, crystalline monolayers. In addition, the Langmuir-Schaefer technique works better than drop casting as particles were packed over larger areas. From the TEM image of particles dispersed in pure chloroform, the average size of the nanocubes was determined to be 14.2 ± 4.0 nm. This means that the particles are very close to the superparamagnetic limit of iron which is approximately 6 nm. This could be confirmed using a neodymium magnet that showed that in the presence of an external magnetic field the nanocubes could be magnetized. Thermal decomposition of iron acetylacetonate can therefore be successfully used to synthesize nanocubes with a narrow size distribution.

From the pressure-area isotherms obtained from the Langmuir-Schaefer technique, it could be determined that particles dispersed in choroform:methanol 3:1, 4:1 and also pure chloroform, have high compressibility. This means that

these particles would be able to form thin crystalline packing during monolayer formation. This could be confirmed from the images obtained from TEM.

In addition to using drop casting and Langmuir-Schaefer technique for the deposition of the iron oxide nanocubes on the substrate, other deposition techniques can be used for the preparation of samples such as spin coating and Langmuir-Blodgett as discussed previously. The LB technique is able to produce structurally ordered monolayers of nanoparticles with good crystalline packing.[26] Since the success of samples prepared using the Langmuir trough rely heavily on the dispersing agent used, other mixed solvent systems can also be studied apart from chloroform and methanol. Since the thermal decomposition for the synthesis of iron oxide cubes depends on a number of factors such as temperature of decomposition, concentration of surfactants, etc, these factors affecting the synthesis could be varied to determine how changing the synthesis conditions affect the shape, size and crystallinity of the synthesize nanocubes. Multiple syntheses using different surfactants, such as oleic acid, lauric acid and octanoic acid could be carried out in order to determine how changing the carbon chain length of the surfactant affects the relative packing of the nanocubes. From the TEM images obtained for uniformly packed nanocubes, spacing between the nanocubes can also be measured to understand the coating mechanism of the surfactants.

REFERENCES

1) Laurent, S.; Delphine, F.; Marc, P.; Alain, R.; Caroline, R.; Luce, V. E.; Robert, N.M.*Chem. Rev.* **2008,** *108,* 2064-2110.

2) Wu, W.; He, Q.; Jiang, C. *Nanoscale. Res. Lett.* **2008,** *3,* 397-415.

3) Yin, M.; Willis, A.; Redl, F.; Turro, N. J.; O'Brien, S. P. *J. Mater. Res.* **2004,** *19(4),* 1208-1215.

4) Miessler, G. L.; Tarr, D. A. *Inorganic Chemistry,* 3rd ed.; Pearson/Prentice Hall: Northfield, Minnesota, 2003.

5) Binns, C. *Introduction to Nanoscience and Nanotechnology,* 1st ed.; Wiley: Hoboken, New Jersey, 2010.

6) Lu, A. H.; Salabas, E. L.; Schuth, F. *Angew. Chem. Int. Ed.* **2007**, *46 (8),* 1222-1244.

7) Baoliang, L.; Xu, Y.; Wu, D.; Sun, Y.; *Particuology*. **2008**, *6,* 334–339.

8) Lee, J. S.; Cha, J. M.; Yoon, H. Y.; Lee, J; Kim, Y. K.; *Sci. Rep.* **2015**, *5(12135)*.

9) Kneller, E. F.; Luborsky, F. E.; *Appl. Phys.*, **1963**, *34*, 656-658.

10) Babes, L.; Denizot, B.; Tanguy, G.; Le Jeune, J. J.; Jallet, P. *J. Coll. Int. Sci.* **1999,** *212,* 474-482.

11) Cornelis, K.; Hurlburt C. S. *Manual of Mineralogy,* 19th ed.; Wiley: New York, 1977.

12) Friák, M.; Schindlmayr, A.; Scheffler, M.; *New J. Phys.* **2007,** *9,* 5.

13) Guardia, P.; Labarta, A.; Batlle, X. *J. Phys. Chem. C.* **2011,** *115(2)*, 390-396.

14) Singh, G.; Chan, H; Baskin, A; Gelman, E; Repnin, N; Král, P; Klajn, R, *Science*, *345 (6201),* 1149-1153.

15) Cavallini, M. *Phys. Chem. Chem. Phys.* **2012,** *14,* 11867-11876.

16) Edwards, K. B.A. Thesis, Mount Holyoke College, 2013.

17) Feng, V. B.A. Thesis, Mount Holyoke College, 2016.

18) Gupta, A. K.; Gupta, M. *Biomaterials.* **2005,** *26*, 3995-4021.

19) Li, Y.; Liu, J.; Wang, Y.; Wang, Z. L. *Chem. Mater.* **2001,** *13(3)*, 1008-1014.

20) Cheung, C. L.; Kurtz, A.; Park, H.; Lieber, C. M. *J. Phys. Chem. B.* **2002,** *106(10)*, 2429-2433.

21) Hyeon, T.; Lee, S. S.; Park, J.; Chung, Y.; Na, H. B. *J. Am. Chem. Soc.* **2001,** *123(51)*, 12798-12801.

22) Jana, N.R; Chen, Y.;Peng, X; *Chem. of Mat.* **2004,** *16 (20),* 3931-5.

23) Laurell Technologies. What is spin coating
http://www.spincoater.com/what-is-spin-coating.php
(accessed Nov 4, 2016).

24) Biolin Scientific. Langmuir-Schaefer Film.
http://www.biolinscientific.com/application/langmuir-schaefer-film/
(accessed Nov 4, 2016).

25) Lee, D. K.; Young H. K.; Chang, W. K.; Hyun, G. C.; Young, S. Kang. *J. Phys. Chem. B.* **2007**, *111(31)*, 9288-9293.

26) Glossary of Nanotechnology and Related Terms. Langmuir-Blodgett method. http://eng.thesaurus.rusnano.com/wiki/article1797?sphrase_id=37 (accessed Mar 28, 2016).

27) Wang, X.; Zhuang, J.; Peng, Q.; Li, Y., *Nature.* **2005**, 437 (7055), 121-4.

28) Guardia, P.; Pérez, N.; Labarta, A.; Batlle, X. *Langmuir.* **2010,** *26(8)*, 5843-5847.

29) Encyclopedia Britannica. Transmission electron microscope (TEM). http://media-2.web.britannica.com/eb-media/90/113690-004-CB552E7F.jpg (accessed Feb 28, 2017).

30) Sun, S. H.; Anders, S.; Hamann, H. F.; Thiele, J. U.; Baglin, J. E. E.; Thomson, T.; Fullerton, E. E.; Murray, C. B.; Terris, B. D. *J. Am. Chem. Soc.* **2002**, *124*, 2884-2885.

31) Kim, B. H.; Shin, K.; Kwon, S. G.; Jang, Y.; Lee, H. S.; Lee, H.; Jun, S.W.; Lee, J.; Han, S. Y.; Yim, Y.

32) Corricelli, M; Altamura,D; De Caro, L; Guagliardi, A; Falqui, A; Genovese, A; Agostiano, A; Giannini, C; Striccoli, Curri, M. L; *CrystEngComm*, **2011**, 13, 3988-3997.

33) Losche, M.; Helm, C.; Mattes, H. D.; Mohwald, H. *Thin Solid Films,* **1985,** *133*, 51.

34) Orbulescu, J.; Mello, S. V.; Huo, Q.; Sui, G.; Kele, P.; Leblanc, R. M. *Langmuir.* **2001,** *17,* 1525-1528.

35) Marcus, Y. *J. Chem. Soc. Faraday Trans. 1,* **1988,** *84(5),* 1465-1473.

36) Ashwell, G. J.; Handa, T.; Jefferies, G.; Hamilton, D. G. *Colloids Surf., A.* **1995,** *102,* 133-136.

37) Peter R. Griffiths, J. A. D. H., Fourier Transform Infrared Spectrometry. Second Edition ed.; Wiley-Interscience; p 560-570, 2007.

38) Signorini, L.; Pasquini, L.; Savini, L.; Carboni, R.; Federico, B.; Bonetti, E.; Giglia, A.; Pedio, M.; Mahne, N.; Nannarone, S. *Phys. Rev. B.* **2003,** *68,* 195423.

39) Bronstein, L. M.; Huang, X.; Retrum, J.; Schemucker, A.; Pink, M.; Stein, B. D.; Dragnea, B. *Chem. Mater.* **2007,** *19,* 3624-3632.

40) Lambert, J. B.; Shurvell, H. F.; Cooks, R. G. *Introduction to Organic Spectroscopy,* 1st ed.; Macmillan Publication: New York, 1987.